early detection by providing an indirect means to monitor changes in gene and microRNA expression in the liver.

Conflicts of interest

None.

Acknowledgments

This work was supported by Grants-in-Aid for scientific research and development from the Ministry of Health, Labor and Welfare and Ministry of Education Culture Sports Science and Technology, Government of Japan. No writing assistance was provided for this manuscript.

Appendix A. Supplementary data

Supplementary data related to this article can be found at doi:10.1016/j.jinf.2014.10.017.

References

1. Fields BN, Knipe DM, Howley PM. *Fields virology*. 5th ed. Philadelphia: Wolters Kluwer Health/Lippincott Williams & Wilkins; 2007.
2. McMahon BJ. The natural history of chronic hepatitis B virus infection. *Hepatology* 2009 May;**49**(5 Suppl):S45–55 [Consensus Development Conference, NIH Research Support, U.S. Gov't, P.H.S.].
3. Brechot C, Kremsdorf D, Soussan P, Pineau P, Dejean A, Paterlini-Brechot P, et al. Hepatitis B virus (HBV)-related hepatocellular carcinoma (HCC): molecular mechanisms and novel paradigms. *Pathol Biol (Paris)* 2010 Aug;**58**(4):278–87 [Review].
4. Xi Y, Nakajima G, Gavin E, Morris CG, Kudo K, Hayashi K, et al. Systematic analysis of microRNA expression of RNA extracted from fresh frozen and formalin-fixed paraffin-embedded samples. *RNA* 2007 Oct;**13**(10):1668–74 [Research Support, N.I.H., Extramural].
5. Liu AM, Zhang C, Burchard J, Fan ST, Wong KF, Dai H, et al. Global regulation on microRNA in hepatitis B virus-associated hepatocellular carcinoma. *Omics* 2011 Mar;**15**(3):187–91.
6. Bala S, Marcos M, Szabo G. Emerging role of microRNAs in liver diseases. *World J Gastroenterol* 2009 Dec 7;**15**(45):5633–40 [Research Support, N.I.H., Extramural Research Support, Non-U.S. Gov't Review].
7. Ji F, Yang B, Peng X, Ding H, You H, Tien P. Circulating microRNAs in hepatitis B virus-infected patients. *J Viral Hepat* 2011 Jul;**18**(7):e242–51 [Research Support, Non-U.S. Gov't].
8. Mitchell PS, Parkin RK, Kroh EM, Fritz BR, Wyman SK, Pogosova-Agadjanyan EL, et al. Circulating microRNAs as stable blood-based markers for cancer detection. *Proc Natl Acad Sci U. S. A.* 2008 Jul 29;**105**(30):10513–8 [Research Support, N.I.H., Extramural Research Support, Non-U.S. Gov't].
9. Ura S, Honda M, Yamashita T, Ueda T, Takatori H, Nishino R, et al. Differential microRNA expression between hepatitis B and hepatitis C leading disease progression to hepatocellular carcinoma. *Hepatology* 2009 Apr;**49**(4):1098–112.
10. Hayes CN, Akamatsu S, Tsuge M, Miki D, Akiyama R, Abe H, et al. Hepatitis B virus-specific miRNAs and argonaute2 play a role in the viral life cycle. *PLoS One* 2012;**7**(10):e47490 [Research Support, Non-U.S. Gov't].
11. Shwetha S, Gouthamchandra K, Chandra M, Ravishankar B, Khaja MN, Das S. Circulating miRNA profile in HCV infected serum: novel insight into pathogenesis. *Sci Rep* 2013 Apr;**3**(3):1555 [Research Support, Non-U.S. Gov't].
12. Turchinovich A, Weiz L, Langheinz A, Burwinkel B. Characterization of extracellular circulating microRNA. *Nucleic Acids Res* 2011 Sep 1;**39**(16):7223–33 [Research Support, Non-U.S. Gov't].
13. Arroyo JD, Chevillet JR, Kroh EM, Ruf IK, Pritchard CC, Gibson DF, et al. Argonaute2 complexes carry a population of circulating microRNAs independent of vesicles in human plasma. *Proc Natl Acad Sci U. S. A* 2011 Mar 22;**108**(12):5003–8 [Research Support, N.I.H., Extramural Research Support, Non-U.S. Gov't].
14. Novellino L, Rossi RL, Bonino F, Cavallone D, Abrignani S, Pagani M, et al. Circulating hepatitis B surface antigen particles carry hepatocellular microRNAs. *PLoS One* 2012;**7**(3):e31952.
15. Gallo A, Tandon M, Alevizos I, Illei GG. The majority of microRNAs detectable in serum and saliva is concentrated in exosomes. *PLoS One* 2012;**7**(3):e30679 [Comparative Study Research Support, N.I.H., Intramural].
16. Huang X, Yuan T, Tschannen M, Sun Z, Jacob H, Du M, et al. Characterization of human plasma-derived exosomal RNAs by deep sequencing. *BMC Genomics* 2013;**14**:319 [Research Support, N.I.H., Extramural Research Support, Non-U.S. Gov't].
17. Conde-Vancells J, Rodriguez-Suarez E, Embade N, Gil D, Matthiesen R, Valle M, et al. Characterization and comprehensive proteome profiling of exosomes secreted by hepatocytes. *J Proteome Res* 2008 Dec;**7**(12):5157–66 [Research Support, N.I.H., Extramural Research Support, Non-U.S. Gov't].
18. Li J, Liu K, Liu Y, Xu Y, Zhang F, Yang H, et al. Exosomes mediate the cell-to-cell transmission of IFN-alpha-induced antiviral activity. *Nat Immunol* 2013 Aug;**14**(8):793–803 [Research Support, Non-U.S. Gov't].
19. Desmet VJ, Gerber M, Hoofnagle JH, Manns M, Scheuer PJ. Classification of chronic hepatitis: diagnosis, grading and staging. *Hepatology* 1994 Jun;**19**(6):1513–20 [Review].
20. Dweep H, Sticht C, Pandey P, Gretz N. miRWalk–database: prediction of possible miRNA binding sites by "walking" the genes of three genomes. *J Biomed Inf* 2011 Oct;**44**(5):839–47 [Research Support, Non-U.S. Gov't].
21. Mathivanan S, Fahner CJ, Reid GE, Simpson RJ. ExoCarta 2012: database of exosomal proteins, RNA and lipids. *Nucleic Acids Res* 2012 Jan;**40**(Database issue):D1241–4 [Research Support, Non-U.S. Gov't].
22. Vartanian JP, Henry M, Marchio A, Suspene R, Aynaud MM, Guetard D, et al. Massive APOBEC3 editing of hepatitis B viral DNA in cirrhosis. *PLoS Pathog* 2010 May;**6**(5):e1000928 [Research Support, Non-U.S. Gov't].
23. Yang JH, Li JH, Jiang S, Zhou H, Qu LH. ChIPBase: a database for decoding the transcriptional regulation of long non-coding RNA and microRNA genes from ChIP-Seq data. *Nucleic Acids Res* 2013 Jan;**41**(Database issue):D177–87 [Research Support, Non-U.S. Gov't].
24. Lum G, Gambino SR. Serum gamma-glutamyl transpeptidase activity as an indicator of disease of liver, pancreas, or bone. *Clin Chem* 1972 Apr;**18**(4):358–62.
25. Bala S, Petrasek J, Mundkur S, Catalano D, Levin I, Ward J, et al. Circulating microRNAs in exosomes indicate hepatocyte injury and inflammation in alcoholic, drug-induced, and inflammatory liver diseases. *Hepatology* 2012 Nov;**56**(5):1946–57 [Research Support, N.I.H., Extramural].
26. Arataki K, Hayes CN, Akamatsu S, Akiyama R, Abe H, Tsuge M, et al. Circulating microRNA-22 correlates with microRNA-122

Please cite this article in press as: Akamatsu S, et al., Differences in serum microRNA profiles in hepatitis B and C virus infection, J Infect (2014), http://dx.doi.org/10.1016/j.jinf.2014.10.017

and represents viral replication and liver injury in patients with chronic hepatitis B. *J Med Virology* 2013 May;**85**(5): 789–98 [Research Support, Non-U.S. Gov't].
27. Wang S, Qiu L, Yan X, Jin W, Wang Y, Chen L, et al. Loss of MiR-122 expression in patients with hepatitis B enhances hepatitis B virus replication through cyclin G1 modulated P53 activity. *Hepatology* 2012 Mar;**55**(3):730–41.
28. Hu J, Xu Y, Hao J, Wang S, Li C, Meng S. MiR-122 in hepatic function and liver diseases. *Protein Cell* 2012 May;**3**(5): 364–71.
29. Chang J, Nicolas E, Marks D, Sander C, Lerro A, Buendia MA, et al. miR-122, a mammalian liver-specific microRNA, is processed from hcr mRNA and may downregulate the high affinity cationic amino acid transporter CAT-1. *RNA Biol* 2004 Jul;**1**(2): 106–13 [Research Support, N.I.H., Extramural Research Support, Non-U.S. Gov't].
30. Chen Y, Shen A, Rider PJ, Yu Y, Wu K, Mu Y, et al. A liver-specific microRNA binds to a highly conserved RNA sequence of hepatitis B virus and negatively regulates viral gene expression and replication. *Faseb J* 2011 Dec;**25**(12):4511–21.
31. Qiu L, Fan H, Jin W, Zhao B, Wang Y, Ju Y, et al. miR-122-induced down-regulation of HO-1 negatively affects miR-122-mediated suppression of HBV. *Biochem Biophys Res Commun* 2010 Aug 6;**398**(4):771–7 [Research Support, Non-U.S. Gov't].
32. Potenza N, Papa U, Mosca N, Zerbini F, Nobile V, Russo A. Human microRNA hsa-miR-125a-5p interferes with expression of hepatitis B virus surface antigen. *Nucleic Acids Res* 2011 Jul; **39**(12):5157–63.
33. Zhang GL, Li YX, Zheng SQ, Liu M, Li X, Tang H. Suppression of hepatitis B virus replication by microRNA-199a-3p and microRNA-210. *Antivir Res* 2010 Nov;**88**(2):169–75 [Research Support, Non-U.S. Gov't].
34. Li D, Liu X, Lin L, Hou J, Li N, Wang C, et al. MicroRNA-99a inhibits hepatocellular carcinoma growth and correlates with prognosis of patients with hepatocellular carcinoma. *J Biol Chem* 2011 Oct 21;**286**(42):36677–85 [Research Support, Non-U.S. Gov't].
35. Takata A, Otsuka M, Kojima K, Yoshikawa T, Kishikawa T, Yoshida H, et al. MicroRNA-22 and microRNA-140 suppress NF-kappaB activity by regulating the expression of NF-kappaB coactivators. *Biochem Biophys Res Commun* 2011 Aug 12;**411**(4):826–31 [Research Support, Non-U.S. Gov't].
36. Xu D, Takeshita F, Hino Y, Fukunaga S, Kudo Y, Tamaki A, et al. miR-22 represses cancer progression by inducing cellular senescence. *J Cell Biol* 2011 Apr 18;**193**(2):409–24 [Research Support, Non-U.S. Gov't].
37. Shi C, Xu X. MicroRNA-22 is down-regulated in hepatitis B virus-related hepatocellular carcinoma. *Biomed Pharmacother* 2013 Jun;**67**(5):375–80 [Research Support, Non-U.S. Gov't].
38. Bandiera S, Ruberg S, Girard M, Cagnard N, Hanein S, Chretien D, et al. Nuclear outsourcing of RNA interference components to human mitochondria. *PLoS One* 2011;**6**(6): e20746.
39. D'Agostino DM, Bernardi P, Chieco-Bianchi L, Ciminale V. Mitochondria as functional targets of proteins coded by human tumor viruses. *Adv Cancer Res* 2005;**94**:87–142.
40. Li LZ, Zhang CZ, Liu LL, Yi C, Lu SX, Zhou X, et al. miR-720 inhibits tumor invasion and migration in breast cancer by targeting TWIST1. *Carcinogenesis* 2014 Feb;**35**(2):469–78 [Comparative Study Research Support, Non-U.S. Gov't].
41. Schopman NC, Heynen S, Haasnoot J, Berkhout B. A miRNA-tRNA mix-up: tRNA origin of proposed miRNA. *RNA Biol* 2010 Sep-Oct;**7**(5):573–6 [Research Support, Non-U.S. Gov't].
42. Ou JH, Laub O, Rutter WJ. Hepatitis B virus gene function: the precore region targets the core antigen to cellular membranes and causes the secretion of the e antigen. *Proc Natl Acad Sci U. S. A* 1986 Mar;**83**(6):1578–82 [Research Support, U.S. Gov't, P.H.S.].
43. Garcia PD, Ou JH, Rutter WJ, Walter P. Targeting of the hepatitis B virus precore protein to the endoplasmic reticulum membrane: after signal peptide cleavage translocation can be aborted and the product released into the cytoplasm. *J Cell Biol* 1988 Apr;**106**(4):1093–104 [Research Support, Non-U.S. Gov't Research Support, U.S. Gov't, P.H.S.].
44. Milich D, Liang TJ. Exploring the biological basis of hepatitis B e antigen in hepatitis B virus infection. *Hepatology* 2003 Nov; **38**(5):1075–86 [Review].
45. Lang T, Lo C, Skinner N, Locarnini S, Visvanathan K, Mansell A. The hepatitis B e antigen (HBeAg) targets and suppresses activation of the toll-like receptor signaling pathway. *J Hepatol* 2011 Oct;**55**(4):762–9 [Research Support, Non-U.S. Gov't].
46. Wu S, Kanda T, Imazeki F, Nakamoto S, Tanaka T, Arai M, et al. Hepatitis B virus e antigen physically associates with receptor-interacting serine/threonine protein kinase 2 and regulates IL-6 gene expression. *J Infect Dis* 2012 Aug 1; **206**(3):415–20 [Research Support, Non-U.S. Gov't].
47. Tong S, Kim KH, Chante C, Wands J, Li J. Hepatitis B Virus e Antigen Variants. *Int J Med Sci* 2005;**2**(1):2–7.
48. Nguyen DH, Hu J. Reverse transcriptase- and RNA packaging signal-dependent incorporation of APOBEC3G into hepatitis B virus nucleocapsids. *J Virol* 2008 Jul;**82**(14):6852–61 [Research Support, N.I.H., Extramural].
49. Warner BG, Abbott WG, Rodrigo AG. Frequency-dependent selection drives HBeAg seroconversion in chronic hepatitis B virus infection. *Evol Med Public Health* 2014 Jan;**2014**(1): 1–9.
50. Winther TN, Bang-Berthelsen CH, Heiberg IL, Pociot F, Hogh B. Differential plasma microRNA profiles in HBeAg positive and HBeAg negative children with chronic hepatitis B. *PLoS One* 2013;**8**(3):e58236 [Research Support, Non-U.S. Gov't].
51. Johnston M, Geoffroy MC, Sobala A, Hay R, Hutvagner G. HSP90 protein stabilizes unloaded argonaute complexes and microscopic P-bodies in human cells. *Mol Biol Cell* 2010 May 1;**21**(9):1462–9 [Research Support, Non-U.S. Gov't].
52. Shim HY, Quan X, Yi YS, Jung G. Heat shock protein 90 facilitates formation of the HBV capsid via interacting with the HBV core protein dimers. *Virology* 2011 Feb 5;**410**(1):161–9 [Research Support, Non-U.S. Gov't].
53. Liu C, Zhang X, Huang F, Yang B, Li J, Liu B, et al. APOBEC3G inhibits microRNA-mediated repression of translation by interfering with the interaction between Argonaute-2 and MOV10. *J Biol Chem* 2012 Aug 24;**287**(35):29373–83 [Research Support, N.I.H., Extramural sResearch Support, Non-U.S. Gov't].
54. Zhao D, Wang X, Lou G, Peng G, Li J, Zhu H, et al. APOBEC3G directly binds Hepatitis B virus core protein in cell and cell free systems. *Virus Res* 2010 Aug;**151**(2):213–9 [Research Support, Non-U.S. Gov't].
55. Gibbings DJ, Ciaudo C, Erhardt M, Voinnet O. Multivesicular bodies associate with components of miRNA effector complexes and modulate miRNA activity. *Nat Cell Biol* 2009 Sep; **11**(9):1143–9 [Comment Research Support, Non-U.S. Gov't].
56. Li J, Liu Y, Wang Z, Liu K, Wang Y, Liu J, et al. Subversion of cellular autophagy machinery by hepatitis B virus for viral envelopment. *J Virol* 2011 Jul;**85**(13):6319–33 [Research Support, Non-U.S. Gov't].

Please cite this article in press as: Akamatsu S, et al., Differences in serum microRNA profiles in hepatitis B and C virus infection, J Infect (2014), http://dx.doi.org/10.1016/j.jinf.2014.10.017

Research Article

Journal of Innate Immunity

J Innate Immun 2015;7:47–58
DOI: 10.1159/000365113

Received: March 14, 2014
Accepted after revision: June 9, 2014
Published online: August 8, 2014

A MAVS/TICAM-1-Independent Interferon-Inducing Pathway Contributes to Regulation of Hepatitis B Virus Replication in the Mouse Hydrodynamic Injection Model

Chean Ring Leong[a] Hiroyuki Oshiumi[a] Masaaki Okamoto[a] Masahiro Azuma[a] Hiromi Takaki[a] Misako Matsumoto[a] Kazuaki Chayama[b] Tsukasa Seya[a]

[a]Department of Microbiology and Immunology, Graduate School of Medicine, Hokkaido University, Sapporo, and [b]Department of Gastroenterology and Metabolism, Applied Life Sciences, Institute of Biomedical and Health Sciences, Hiroshima University, Hiroshima, Japan

Key Words

Type I interferon · Hepatitis B virus regulation · Toll/IL-1R homology domain-containing adaptor molecule 1 · Mitochondrial antiviral signaling protein · Pathogen-associated molecular patterns

Abstract

Toll-like receptors (TLRs) and cytoplasmic RNA sensors have been reported to be involved in the regulation of hepatitis B virus (HBV) replication, but remain controversial due to the lack of a natural infectious model. Our current study sets out to characterize aspects of the role of the innate immune system in eliminating HBV using hydrodynamic-based injection of HBV replicative plasmid and knockout mice deficient in specific pathways of the innate system. The evidence indicated that viral replication was not affected by MAVS or TICAM-1 knockout, but absence of interferon regulatory factor 3 (IRF-3) and IRF-7 transcription factors, as well as the interferon (IFN) receptor, had an adverse effect on the inhibition of HBV replication, demonstrating the dispensability of MAVS and TICAM-1 pathways in the early innate response against HBV. *Myd88*$^{-/-}$ mice did not have a significant increase in the initial viremia, but substantial viral antigen persisted in the mice sera, a response similar to *Rag2*$^{-/-}$ mice, suggesting that the MyD88-dependent pathway participated in evoking an adaptive immune response against the clearance of intrahepatic HBV. Taken together, we show that the RNA-sensing pathways do not participate in the regulation of HBV replication in a mouse model; meanwhile MyD88 is implicated in the HBV clearance.

Introduction

Hepatitis B virus (HBV) is a noncytopathic human DNA (hepadna) virus that infects hepatocytes causing acute and chronic hepatitis [1]. More than 360 million people are chronically infected with HBV worldwide. Although less than 5% of HBV-infected patients develop persistent infections that progress to liver cirrhosis and hepatocellular carcinoma, HBV causes about 20% of hepatocellular carcinoma deaths [2]. The adaptive immune response is widely acknowledged as pivotal in the defense against HBV. However, the role of innate immunity during HBV infection remains controversial since analysis in patients at the early stage of infection is unfeasible. In ad-

1662–811X/14/0071–0047$39.50/0

E-Mail karger@karger.com
www.karger.com/jin

Dr. Tsukasa Seya
Department of Microbiology and Immunology
Graduate School of Medicine, Hokkaido University
Kita-15, Nishi-7, Kita-ku, Sapporo 060-8638 (Japan)
E-Mail seya-tu@pop.med.hokudai.ac.jp

dition, no reliable cell-based in vitro infection system or convenient animal model is available.

During HBV infection, the HBV genome is delivered into the nucleus. Infection is defined by the formation of covalently closed circular DNA. Following formation of covalently closed circular DNA, viral mRNA and pregenomic RNA are transcribed [3, 4]. The pregenomic RNA is subsequently converted to a partially double-stranded genome by the viral DNA polymerase. Unlike other DNA viruses, HBV uses an RNA proviral intermediate that must be copied back into DNA for replication. Although these replication steps are sequestered in the nucleus of infected cells, cytoplasmic DNA/RNA sensors are reported to affect the efficacy of HBV replication [5, 6]. The association between cytoplasmic pattern recognition receptors and the dynamics of the HBV life cycle in HBV-infected cells needs to be clarified.

Viral RNA is sensed by the innate immune system by either Toll-like receptor 3 (TLR3) or cytoplasmic sensors such as retinoic acid-inducible gene-I (RIG-I) and melanoma differentiation-associated gene 5 (MDA5). RIG-I and MDA5 mainly participate in type I interferon (IFN) induction in conjunction with the adaptor molecule, mitochondrial antiviral signaling protein (MAVS; also called IPS-1, Cardif, or VISA) [7–9]. The Toll/IL-1R homology domain-containing adaptor molecule 1 (TICAM-1; also called TRIF) is the adaptor of TLR3, which senses viral RNA on the endosomal membrane [8–10]. Several DNA sensors, most of which signal through STING for type I IFN induction, have been reported in recent years [11]. A few reports have also mentioned that MAVS participates in DNA sensing in certain human cells whereby poly-dA/dT DNA is found to signal via RIG-I. Later, it was also shown that poly-dA/dT serves as a template for RNA polymerase III to make RIG-I ligands [12–14]. Nevertheless, this hypothesis is unresolved in mouse cells. Once stimulated by the viral DNA/RNA, these adaptor proteins activate IFN regulatory factor (IRF)-3 and IRF-7, which induce type I IFN production [7–9]. These pattern recognition receptor-mediated early innate immune responses are crucial in controlling viral replication and spread before the initiation of more specific and powerful adaptive immune responses [8, 9, 15].

Despite numerous studies on HBV pathogenesis, the putative molecular patterns of HBV that trigger cellular responses remain unknown. A few reports have suggested that the antiviral response against HBV is mediated by the RIG-I/MAVS pathway in the cytosol and its activation is blocked by HBV polymerase in infected cells [16–18]. However, no definitive evidence in vivo is available because analysis on the gene expression and effectors required for elimination of the replicative template has been especially difficult. Since viral clearance is a multifaceted process, we hydrodynamically injected a naked HBV plasmid DNA into wild-type (WT) and gene-disrupted mice deficient in TICAM-1, MAVS, TICAM-1/MAVS, IRF-3/IRF-7, IFNAR, MyD88, or RAG2 to identify and characterize the immunological events for HBV clearance. With the availability of various gene-disrupted mice, our study allows the identification of pathways crucial for the clearance of HBV.

Materials and Methods

Animal Studies

All mice were backcrossed with C57BL/6 mice more than seven times before use. *Ticam-1*$^{-/-}$ [19] and *Mavs*$^{-/-}$ [20] mice were generated in our laboratory as described previously, while *Ticam-1*$^{-/-}$ *Mavs*$^{-/-}$ mice were generated by crossing *Ticam-1*$^{-/-}$ mice with *Mavs*$^{-/-}$ mice. *Irf-3*$^{-/-}$/*Irf-7*$^{-/-}$ and *Ifnar*$^{-/-}$ mice were kindly provided by T. Taniguchi (University of Tokyo, Tokyo, Japan). *Myd88*$^{-/-}$ mice were provided by Drs. K. Takeda and S. Akira (Osaka University, Osaka, Japan). *Rag2*$^{-/-}$ mice were kindly provided by Dr. N. Ishii (Tohoku University, Sendai, Japan). Female C57BL/6J mice were purchased from CLEA Japan (Tokyo) and used at 7–9 weeks of age. All mice were maintained under specific pathogen-free conditions in the animal facility at Hokkaido University Graduate School of Medicine (Sapporo, Japan). Animal experiments were performed according to the guidelines set by the Animal Safety Center, Japan.

Hydrodynamic Transfection of Mice with HBV1.4 Plasmid

The pTER1.4xHBV plasmid containing 1.4-genome length sequences of HBV that were previously shown to produce a similar sedimentation in sucrose density gradient centrifugation to HBV extracted from the serum of carriers [21] was used in this study. A total of 50 μg of the plasmid was injected into the tail vein of 7- to 9-week-old mice in a volume of 2.0 ml of TransIT-QR hydrodynamic delivery solution (Mirus, USA). The total volume was delivered within 3–8 s. Plasmid DNA was prepared by using an Endo-Free plasmid system (Qiagen, Germany) according to the manufacturer's instructions.

Quantification of HBV DNA by Real-Time PCR

To determine the HBV DNA in the serum, 30 μl of each serum sample was pretreated with 20 units of DNase I (Roche, Germany) at 37°C overnight. The encapsidated viral DNA was extracted with the SMITEST kit (Genome Science Laboratories, Tokyo, Japan) following the manufacturer's instructions and dissolved in 20 μl of TE-buffer. The purified viral genome was quantified by real-time PCR using the SYBR green master mix (Life Technologies, USA) and the HBV-DNA-F/R primer (see suppl. table 1 for primer sequences; for all online suppl. material, see www.karger.com/doi/10.1159/000365113). Amplification conditions included initial denaturation at 95°C for 10 min, followed by 45 cycles of

denaturation at 95°C for 15 s, annealing at 58°C for 5 s, and extension at 72°C for 6 s. The lower detection limit of this assay is 1,000 copies.

Immunohistochemical Staining for HBV Core Antigen

For immunohistochemical staining of the HBV core antigen (HBcAg), mouse livers were fixed with 4% paraformaldehyde overnight, cryoprotected in 30% sucrose, and sectioned at a thickness of 10 μm using Leica cryostat and mounted on Superfrost glass slides. Sections were incubated with the primary antibody (anticore polyclonal rabbit antibody, DAKO) overnight, followed by incubation with an immunoperoxidase technique involving avidin-biotin peroxidase complexes (Vectastain ABC kit; Vector Laboratories, Burlingame, Calif., USA) according to a method reported previously [22].

HBV Surface Antigen Antigenemia

Mice were bled on the days mentioned after injection of pTER-1.4xHBV and serum was isolated by centrifugation. Concentration of HBV surface antigen (HBsAg) in the serum was quantified by sandwich ELISA in commercial ELISA kits following the manufacturer's protocol (XpressBio, USA). The reporting unit is the signal/cutoff ratio of the 1,000-fold diluted serum at an O.D. of 450 nm.

Southern Blotting to Detect Intracapsid HBV DNA

Viral DNA was isolated from intracellular viral capsids and detected with a specific DIG-labeled probe as described previously [21]. In brief, to isolate the viral DNA, mouse livers were homogenized and subjected to overnight sodium dodecyl sulfate-proteinase K digestion followed by phenol extraction and ethanol precipitation. Twenty micrograms of the isolated DNA was separated in 1% agarose gel, transferred onto Immobilon-Ny+ charged nylon membrane (Milipore), and detected with a full-length HBV-DNA probe labeled by the DIG DNA labeling and detection kit (Roche Diagnostics, Basel, Switzerland) according to the instructions provided by the manufacturer.

Anti-HBs Antibody ELISA

IgG antibodies specific for HBsAg were detected by ELISA as described previously [23] with slight modification. A 96-well plate was coated with antigen of HBs in carbonate buffer and followed by blocking of 2% BSA. Plasma samples were diluted 5× and then incubated in the antigen-coated wells for 3 h at room temperature. A horseradish peroxidase-conjugated goat anti-mouse IgGγ (Southern Biotechnology, USA) and TMB were used to develop the signal. Plates were read at 450 nm. Normal mouse plasma was used to generate cutoff values. The antibody titers are reported as the reciprocal of A_{450} (sample)/A_{450} (2.1' normal mouse average) at which samples with a value >1 were considered to have scored positive.

Quantitative HBV or Cytokines mRNA in the Organs

Each organ was extracted from the mice on the days mentioned after hydrodynamic injection of the HBV plasmid. Total RNA of the organs was isolated with TRIzol according to the manufacturer's protocol. Using 0.5–1 μg of total RNA as a template, cDNA was obtained using a high-capacity cDNA transcription kit (Applied Biosystems) according to manufacturer's instructions. qPCR was performed using a Step One real-time PCR system (Applied Biosystems). The expression of cytokine mRNA was normalized to that of β-actin mRNA in each organ, and the fold increase was determined by dividing the expression in each sample by that of the mice receiving the control plasmid. The primer sequences are described in online supplementary table 1.

Quantitative cGAS, STING, and MAVS Expression in Cell Lines

Total RNA was isolated from L929 cells, RAW264.7 cells, immortalized mouse hepatocytes, Huh7 cells, and HepG2 cells with TRIzol according to the manufacturer's protocol. Using 0.5–1 μg of total RNA as a template, cDNA was obtained using a high-capacity cDNA transcription kit (Applied Biosystems) according to manufacturer's instruction. qPCR was performed using a Step One real-time PCR system (Applied Biosystems). The expression of each targeted mRNA was normalized to that of β-actin mRNA in each sample and shown as a relative expression. The primer sequences are described in online supplementary table S1.

Reporter Gene Assay

To prepare the HBV RNA, immortalized mouse hepatocytes previously established in our laboratory [24] were transfected with either control plasmid or pTER1.4xHBV. Total RNA containing the HBV RNA was isolated after 12 h and confirmed with RT-PCR, while the RNA transfected with only control plasmid was used as a control. The isolated RNA was later used as stimuli for the reporter gene assay of IFN-β. Briefly, the immortalized hepatocytes were again transfected with the reporter plasmids. After 16 h, the immortalized hepatocytes were transfected with the stimuli including PIC, a control plasmid, HBV RNA, and pTER1.4xHBV using FuGENE HD (Roche). Cells were lysed at the time point mentioned using a passive lysis buffer, and Firefly and Renilla luciferase activities were determined using a dual-luciferase reporter assay kit. Firefly luciferase activity was normalized by Renilla luciferase activity and was expressed as the fold stimulation relative to activity in nonstimulated cells.

Statistical Analysis

The statistical significance of the obtained data in this study was analyzed using a two-tail unpaired t test and $p < 0.05$ was regarded as statistically significant.

Results

MAVS and TICAM-1 Are Dispensable in Suppressing HBV Replication

We hydrodynamically transfected replication-competent HBV DNA into *Mavs*$^{-/-}$ or *Ticam-1*$^{-/-}$ and *Mavs*$^{-/-}$/*Ticam-1*$^{-/-}$ mice to access the role of these viral RNA-sensing pathways in response to HBV. Serum HBsAg and HBV-DNA levels were monitored regularly as surrogate markers of HBV replication in vivo. WT mice displayed acute self-limiting hepatitis with peak HBs antigenemia on day 4 after DNA injection (fig. 1a–c). Subsequently, HBsAg in sera decreased and terminated by day 11. *Mavs*$^{-/-}$ and *Ticam-1*$^{-/-}$ mice displayed HBsAg clearance

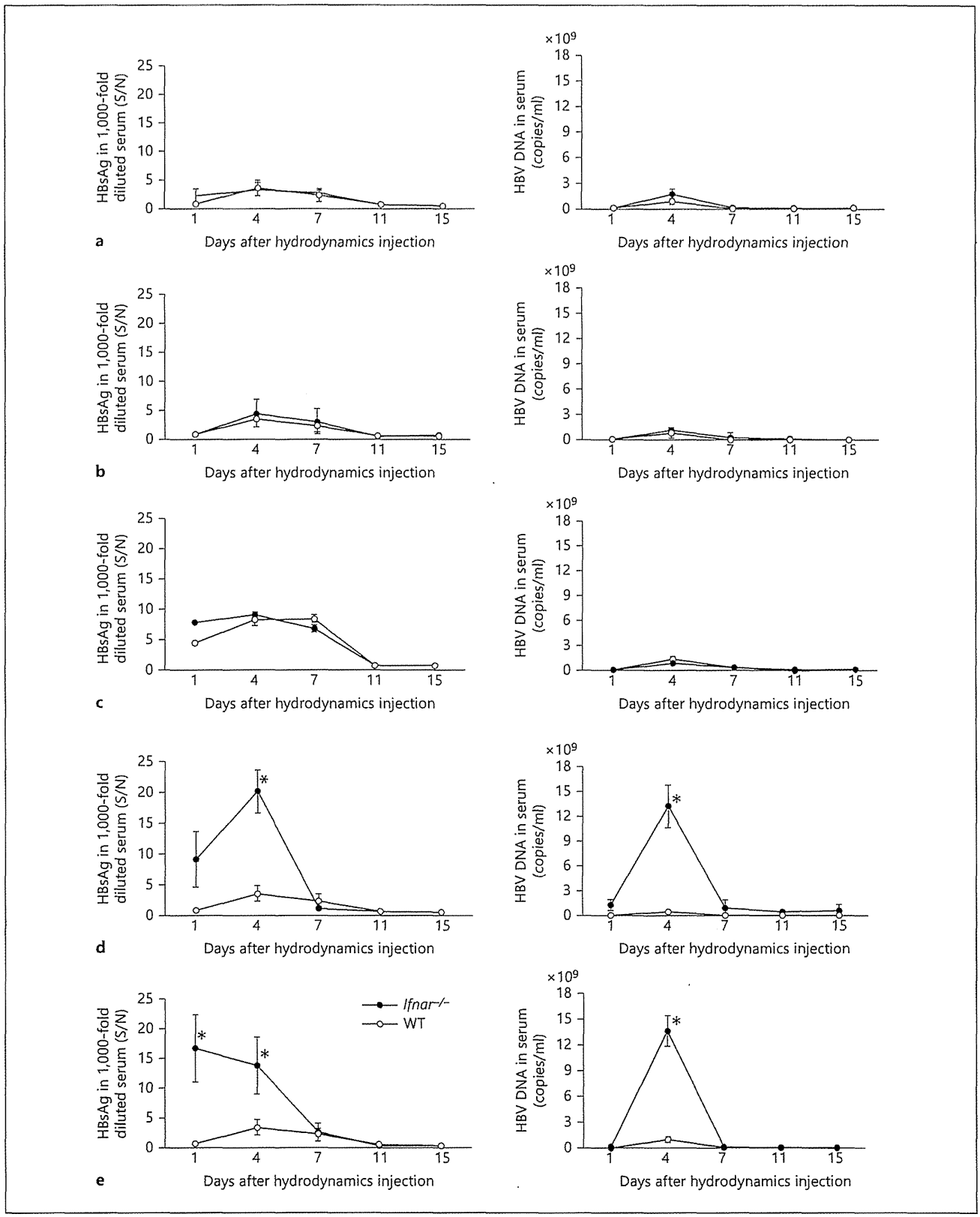

1

(*For legend see next page.*)

J Innate Immun 2015;7:47–58
DOI: 10.1159/000365113

kinetics that closely paralleled the WT mice response (fig. 1a, b, left panels). Serum HBV-DNA levels were quantified using real-time PCR. The average titer of serum HBV DNA in 15 WT mice injected with HBV DNA was below 1×10^4 copies/ml 1 day after injection and reached 2×10^9 copies/ml 4 days after injection (fig. 1a–c, right panels). At later time points, most mice showed no detectable virus titer. Similar results were obtained with *Mavs*$^{-/-}$ and *Ticam-1*$^{-/-}$ mice (fig. 1a, b). The serum HBV-DNA and HBsAg results showed only a marginal effect for the absence of MAVS or TICAM-1 compared to WT mice. The results suggested that the pathways involving these two adaptor proteins were dispensable for triggering the immune responses that suppressed HBV replication.

To determine whether the RIG-I/MDA5-MAVS and TLR3-TICAM-1 RNA-sensing pathways were dispensable for suppressing the HBV replication, similar studies were performed in mice lacking both the MAVS and TICAM-1 adaptor proteins (fig. 1c). No notable differences were observed between WT and MAVS/TICAM-1 double-knockout mice in serum HBsAg and HBV-DNA levels, consistent with other data obtained. In addition, similar kinetics of intrahepatic clearance of the HBV template as well as HBV replication was observed in WT, *Mavs*$^{-/-}$, and *Ticam-1*$^{-/-}$ mice as revealed by Southern blotting using HBV-specific probes (online suppl. fig. 1).

To ensure the efficiency of delivery of the HBV transcriptional template into the mouse liver, a plasmid harboring the *lacZ* gene was used to transfect the liver cells using the hydrodynamic injection method. X-gal (a substrate for *lacZ*) staining showed that nearly the entire liver of injected mice has successfully received the injected plasmid (online suppl. fig. 2). An independent determination of transfection efficiency was carried out using a plasmid harboring the GFP fragment. The comparable transfection efficiencies observed did not differ significantly among the different mouse strains (data not shown). Furthermore, quantification of HBV mRNA in the organs of WT and knockout mice on day 3 after hydrodynamic injection revealed that HBV mRNA was amplified mainly in the liver but not in other organs, including kidney, lung, heart, spleen, and thymus (online suppl. fig. 3). Only weak HBV signals were detected in other organs in some types of knockout mice. These results demonstrated that HBV replication in vivo using the injection method was efficient and liver specific.

To further assess the possibility of HBV RNA acting as pathogen-associated molecular patterns to trigger the induction of type I IFN in hepatocytes, we transfected the immortalized hepatocytes with a plasmid containing the full genome of HBV as well as RNA containing the HBV mRNA. Along with the synthetic analog of dsRNA, poly(I:C), as a control, we determined the activity of the IFN-β promoter upon the stimulation using reporter gene assay (online suppl. fig. 4). Unlike poly(I:C), neither the full genome of HBV nor RNA induced any activity of the type I IFN promoter in the immortalized hepatocytes. Furthermore, we quantified the endogenous expression of genes including *cGas*, *Sting*, and *Mavs* in the hepatocyte cell lines in order to access the intrinsic RNA or DNA-sensing pathways (online suppl. fig. 5). We found that the hepatocyte cell lines, including those originating from mice and humans, expressed extremely low amounts of *Sting* compared to the intrinsic *Mavs*. However, other cell lines, including RAW 264.7 (murine macrophage cell line) and L929 (murine fibrosarcoma cell line), have higher endogenous expression of *Sting* in comparison to *Mavs*.

IRF-3/IRF-7 and IFNAR Are Critical Factors for HBV Replication Regulation

To investigate the mechanisms underlying the rapid termination of HBV replication in WT mice, we examined HBV clearance in IRF-3-/IRF-7-deficient mice. Activation of transcription factors including IRF-3 or IRF-7 is essential for raising immune responses including IFN production [25]. Unlike *Mavs*$^{-/-}$, *Ticam-1*$^{-/-}$, or WT mice, mice lacking the transcription factors IRF-3/IRF-7 had

Fig. 1. IFNAR and IRF-3/IRF-7 are critically associated with regulation of HBV propagation in mice but not MAVS and/or TICAM-1. HBsAg or HBV DNA were measured with sera from *Mavs*$^{-/-}$ (n = 13) (**a**), *Ticam-1*$^{-/-}$ (n = 10) (**b**), *Ticam-1*$^{-/-}$/*Mavs*$^{-/-}$ (n = 6) (**c**), *Irf-3*$^{-/-}$/*Irf-7*$^{-/-}$ (n = 12) (**d**), and *Ifnar*$^{-/-}$ (n = 13) (**e**) mice compared to WT mice (n = 15). These mice were hydrodynamically injected with 50 μg of the pTER-1.4xHBV plasmid containing full-genome HBV DNA. Mouse sera were isolated at the time points indicated. The HBsAg titers in the 1,000-fold diluted serum (left) and HBV DNA (right) in the knockout mice (●) were compared to the WT mice (○). Serum HBsAg titers were determined with an enzyme immunoassay at O.D. 450 nm [calculated as signal-over-noise ratios (S/N)]. Sera HBV DNA were determined by Q-PCR and indicated as copies per milliliter. Error bars indicate SD. The statistical p values were analyzed and no significant differences were observed in **a–c**. * $p < 0.01$ in **d** and **e** are time points statistically different between WT and transgenic mice.

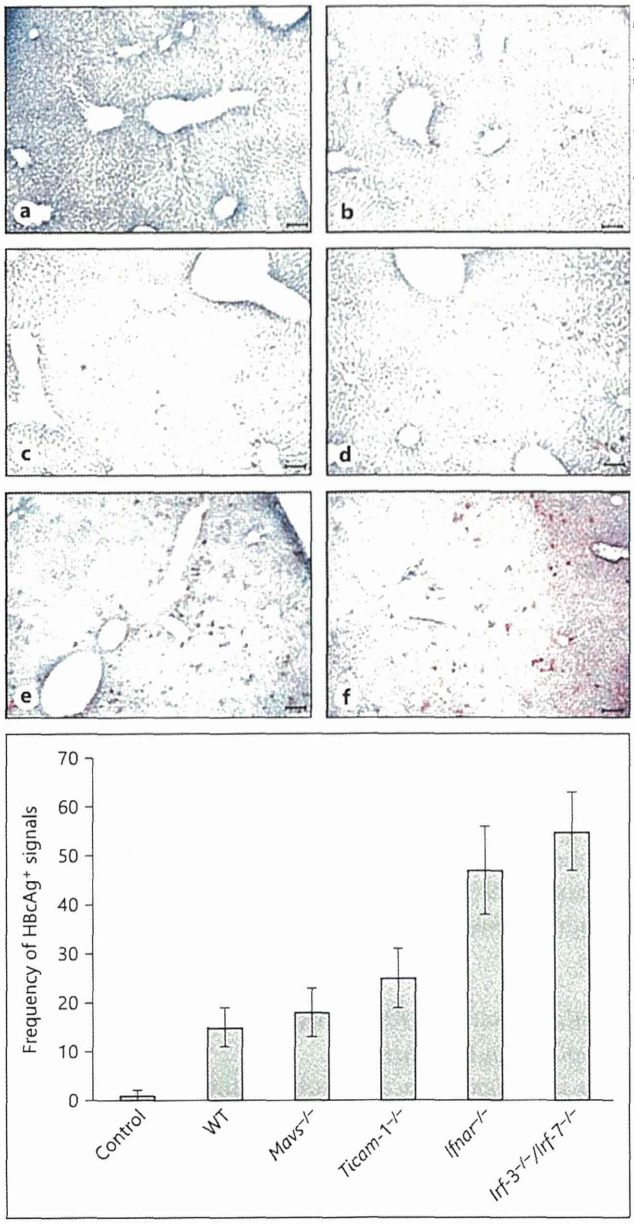

Fig. 2. Lacking IFNAR and IRF-3/IRF-7 causes an increase of HBcAg in mouse liver injected with the HBV replicative plasmid. The HBc protein in the livers on day 3 after injection was visualized with immunohistochemical staining of the mice liver sections embedded in OCT using an anti-HBc antibody for HBcAg. Representative sections are shown. HBcAg-positive cells were absent in the WT mice that received only the control plasmid (**a**). Only marginal differences were observed in the frequency of HBcAg-positive cells between WT (**b**), *Mavs*$^{-/-}$ (**c**), and *TICAM-1*$^{-/-}$ (**d**) mice. Frequency of HBcAg-positive cells in the livers of the *Ifnar*$^{-/-}$ (**e**) and *Irf-3*$^{-/-}$/*Irf-7*$^{-/-}$ (**f**) mice are more prevalent compared to the WT mice. The scale bars represent 10 μm. The images are displayed at 200× magnification. Frequency of HBcAg-positive signals between the different mouse strains shown is based on 3 images of each.

markedly high amounts of HBsAg and HBV DNA in sera (fig. 1d). A sharp peak of HBsAg in sera occurred in *Irf-3*$^{-/-}$/*Irf-7*$^{-/-}$ mice on day 4 after injection. However, in spite of the high virus titer at the early stage, HBsAg and DNA in sera were cleared with kinetics that paralleled the WT mice response, and viremia was eliminated by day 11. Hence, the substantial differences in the serum viremia between WT and *Irf-3*$^{-/-}$/*Irf-7*$^{-/-}$ mice in the early stage after transfection presumably reflects the importance of the genes being expressed with these transcription factors in the suppression of the HBV replication. IRF-3 and IRF-7 are the key molecules in the suppression of HBV viremia in the early stage after HBV injection.

Since type I IFN stimulates the IFNAR pathway to amplify type I IFN production, we hydrodynamically transfected HBV plasmid into mice lacking the gene of the type I IFN receptor (*Ifnar*$^{-/-}$) and assessed the suppression of HBV replication. *Ifnar*$^{-/-}$ mice showed markedly high titers of viral DNA and antigens in sera (fig. 1e) similar to *Irf-3*$^{-/-}$/*Irf-7*$^{-/-}$ mice.

The presence of HBcAg-positive hepatocytes was also monitored by immunohistochemical staining of liver sections from mice of each strain at day 4 after the injections (fig. 2). Data from the observed HBcAg-positive hepatocytes were in good agreement with the results on sera HBsAg and HBV DNA: only deficiency of IRF-3/IRF-7 and IFNAR resulted in a sharp increase of viremia in mice in the early stage (earlier than day 4). Fewer HBcAg-positive hepatocytes were observed in *Mavs*$^{-/-}$ and *Ticam1*$^{-/-}$ as well as WT mice at day 4 after injection than in *Irf-3*$^{-/-}$/*Irf-7*$^{-/-}$ or *Ifnar*$^{-/-}$ mice (fig. 2).

To gain insight into cytokine production in the liver in response to the HBV genome and its replication, we quantified the expression of type I IFN, IFN-γ, IL-7, IL-12p40, and chemokines including CXCL9, CXCL10, and CXCL11 mRNA in the livers of WT mice receiving either the control plasmid or plasmid carrying the HBV full genome on days 1, 3, 7, and 10 after hydrodynamic injection. Replication of HBV in the liver did not cause any significant changes in the expression of the cytokines or chemokines except the IFNs and CXCL-10 (fig. 3a–h). A similar study was carried out in WT and *Ifnar*$^{-/-}$ mice in order to further elaborate the type I IFN production. The IFNs increased in WT mice livers receiving the HBV full genome compared to the mouse livers receiving the control plasmid (fig. 3i–k). This increase was not observed in *Ifnar*$^{-/-}$ mice lacking the INF receptor. Although there appeared to be slight individual-to-individual differences in the apparent peaks of IFN-α induction, the result indicated that IFN-β was responsible for suppressing HBV

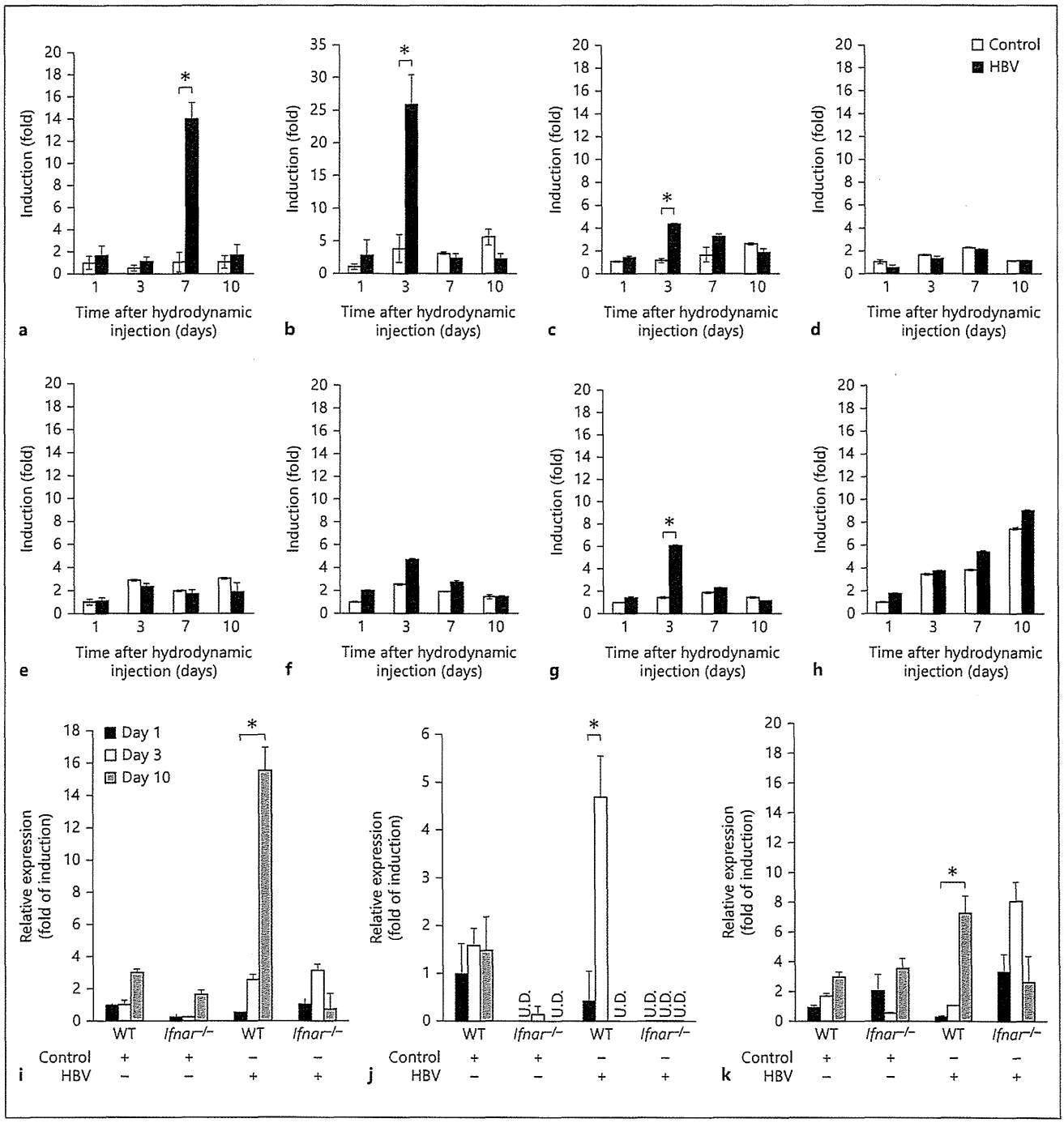

Fig. 3. Type I and II IFN expression is induced by HBV replication, and lacking the type I IFN receptor (IFNAR) causes failure of these inductions. WT mice were hydrodynamically injected with 50 μg of the pTER-1.4xHBV or control plasmid as described, and livers were isolated on days 1, 3, 7, and 10 after injection. The expression of IFN-α (**a**), IFN-β (**b**), IFN-γ (**c**), IL-7 (**d**), IL-12p40 (**e**), CXCL-9 (**f**), CXCL-10 (**g**), and CXCL-11 (**h**) mRNA was determined by reverse transcription followed by real-time PCR, and was expressed as the fold of induction relative to the WT mice receiving the control plasmid. Induction of IFNs and CXCL-10 was observed in the mice receiving the HBV plasmid. Similar studies were conducted in the WT and *Ifnar*$^{-/-}$ mice: IFN-α (**i**), IFN-β (**j**), and IFN-γ (**k**). *Ifnar*$^{-/-}$ mice show reduced expression of the IFNs compared to the WT. Data represent the mean of 3 mice on each strain and time point mentioned. * $p < 0.05$. U.D. = Undetected.

replication early. However, the reason for the lag in the induction of IFN-γ between the WT and *Ifnar*$^{-/-}$ mice remains unclear.

Taken together, these results suggest that type I IFN was indispensable for suppressing HBV replication in the early stage after viral genome entry. Type I IFN binds to its receptor to induce intracellular antiviral proteins to disrupt HBV replication. The results, however, infer that intrahepatic HBV clearance at the later stage is independent of IFN.

HBV Clearance in a Later Stage by Acquired Immunity

Previous studies by Yang et al. [23] and other groups showed that HBV replication persists indefinitely in globally immunodeficient mice such as NOD/Scid mice hydrodynamically injected with the replication-competent plasmid carrying the full genome of HBV. To investigate whether the elevated viral titer in *Ifnar*$^{-/-}$ and *Irf-3*$^{-/-}$/*Irf-7*$^{-/-}$ mice on day 4 after hydrodynamic injection and intrahepatic HBV clearance were related to immune effectors including T and B cells, HBV clearance was examined in *Rag-2*$^{-/-}$ mice. The lack of V(D)J recombination in this strain resulted in failure to produce mature B or T lymphocytes. As shown in figure 4, the absence of mature T and B cells in the *Rag-2*$^{-/-}$ mice did not result in elevated viral titer immediately after transfection, unlike in *Ifnar*$^{-/-}$ and *Irf-3*$^{-/-}$/*Irf-7*$^{-/-}$ mice. However, *Rag-2*$^{-/-}$ mice failed to clear the input plasmid and HBV products, as sera HBsAg and HBV DNA were detected up to day 15 (fig. 4a), by the time viral replication was terminated in all the other strains tested (fig. 4c, d). In other words, activation of the immune effectors such as the B and T cells is responsible for the intrahepatic HBV clearance, their activation being independent of IFN and IRF-3/IRF-7.

MyD88 Deficiency Leads to Slower HBV Clearance

The MyD88-dependent pathway has been known to lead to the production of inflammatory cytokines and is common to all TLRs, except TLR3 [22]. To examine whether a MyD88-dependent pathway is required in the intrahepatic clearance of the HBV, we monitored the serum HBsAg in MyD88-deficient mice. As shown in figure 4b, an increase in sera HBsAg in *Myd88*$^{-/-}$ mice was observed, although without particular antigenemia peaks at the early stage of transfection in *Ifnar*$^{-/-}$ and *Irf-3*$^{-/-}$/*Irf-7*$^{-/-}$ mice (fig. 4b, c). Instead, a delay in the elimination of the HBV was observed (fig. 4b, d). Typically, WT mice or other mouse strains lose serum HBsAg from day 11 after injection. However, serum antigen was detectable on day 15 in *Myd88*$^{-/-}$ mice. Delayed elimination of HBV plasmid and single-strand DNA in the liver was observed in Southern analysis of the liver from *Myd88*$^{-/-}$ mice compared with WT, *Mavs*$^{-/-}$, and *Ticam-1*$^{-/-}$ mice (online suppl. fig. 1).

Additionally, ELISA to determine anti-HBsAg antibody production in mouse sera after hydrodynamic injection revealed that anti-HBs antibody was produced in WT mice from day 7 and peaked at day 15 (fig. 4e). RAG2-deficient mice lacking mature T and B cells failed to produce any antibody, and *Myd88*$^{-/-}$ mice also had lower or nearly undetectable anti-HBs antibody in serum in comparison to the typical response of WT mice at later transfection stages. These results suggested that MyD88 and RAG2 were crucial for triggering acquired immunity against HBV in vivo.

Discussion

In the present study, several different knockout mice were analyzed in an attempt to define the mechanism of innate immunity against HBV in vivo. The evidence we obtained indicated that viral replication was not affected by MAVS or TICAM-1 knockout, but absence of IRF-3 or IRF-7 transcription factors, as well as the IFN receptor, had an adverse effect on the inhibition of HBV replication. The results herein demonstrated that the TICAM-1 and MAVS pathways were not required in either suppressing the virus replication or intrahepatic clearance of HBV replicative plasmid in vivo.

Although a DNA virus, HBV has the unique feature of replicating via an RNA proviral intermediate that is copied into DNA. Thus, defining the virus component, either HBV DNA or RNA that triggers the antiviral response is crucial to understand the immune mechanisms that are responsible for eliminating HBV during infection. HBV RNA has been suggested as the putative pathogen-associated molecular pattern of HBV in a few reports [16–18, 26]. HBx or HBs inhibits IFN-β induction followed by activation of TLR3 or RIG-I pathways with poly(I:C) or SeV, respectively. However, these findings must be interpreted with caution, as poly(I:C) and SeV are heterologous inducers for evaluating either the TLR3 or RIG-I pathway [16, 17]. No definitive conclusion on activation of the TLR3 or RIG-I pathway by HBV RNA in vivo has been reported yet.

Viral RNA is recognized largely by RIG-I or MDA5 in the cytosol of infected cells [27, 28] and by TLR3 or

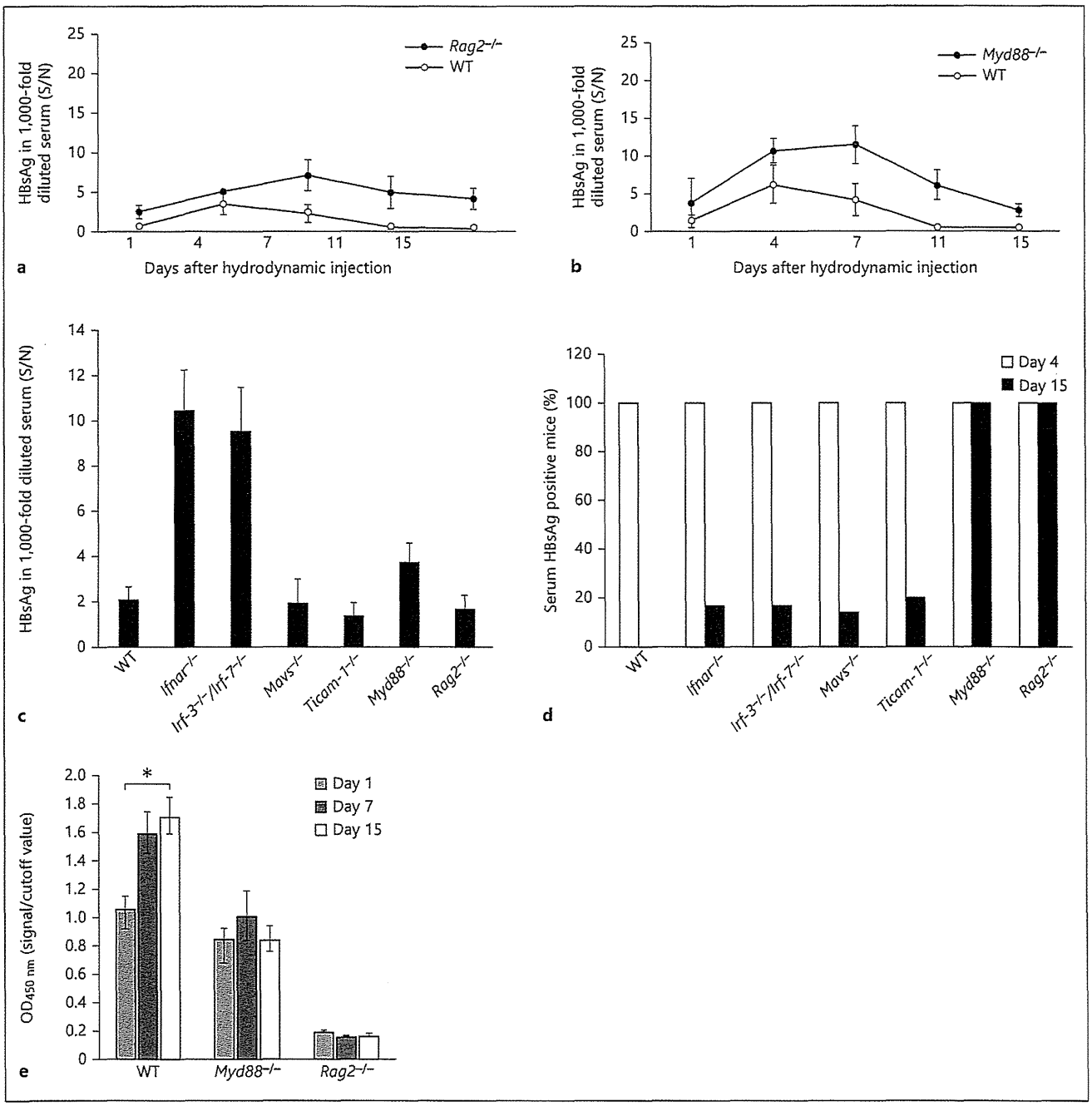

Fig. 4. Mice lacking RAG2 and MyD88 show insufficient clearance of HBV. **a, b** The *Rag2*$^{-/-}$, *Myd88*$^{-/-}$, and WT mice were hydrodynamically injected with 50 μg of pTER-1.4xHBV and HBsAg in the mouse sera at the time points indicated and analyzed with ELISA as described. **c** HBsAg in 1,000-fold diluted serum from all the mice strains including WT, *Ifnar*$^{-/-}$, *Irf-3*$^{-/-}$/*Irf-7*$^{-/-}$, *Mavs*$^{-/-}$, *Ticam-1*$^{-/-}$, *Myd88*$^{-/-}$, and *Rag2*$^{-/-}$ at day 4 after the hydrodynamic injections. Only *Ifnar*$^{-/-}$ and *Irf-3*$^{-/-}$/*Irf-7*$^{-/-}$ mice show a remarkable increase, while a moderate increase of sera HBsAg was seen in *Myd88*$^{-/-}$ mice. **d** HBsAg persistence rates in all the mice strains receiving pTER1.4HBV were determined by the percentage of serum HBsAg-positive mice on day 4 (□) and day 15 (■) after the hydrodynamic injections. Serum HBsAg was found to be persistent only in mice deficient in MyD88 and RAG2 on day 15 as 100% of the mice from these two strains were HBsAg positive (n = 8 for each mice strain). **e** Lacking MyD88 and RAG2 leads to the failure of the knockout mice to produce anti-HBs IgG compared to the WT mice on day 15 after injection as determined by ELISA using antigen of HBs (n = 3 for each mice strain). * $p < 0.05$. S/N = Signal-over-noise ratio.

TLR7/8 in the endosome of other noninfected cells [29, 30]. These RNA sensors require MAVS, TICAM-1, or MyD88 as adaptor proteins to induce type I IFN [28]. On the other hand, cytoplasmic DNA is recognized by DNA sensors including DAI, IFI16, RIG-I, DHX9 (helicase), and cGAS [31]. STING is the only adaptor for all IFN-inducing DNA sensors in mouse cells reported so far [30, 32, 33], although some of these sensors are reported to induce type I IFN via MAVS in human cells. These adaptors, TICAM-1, MAVS, and STING, are all linked to activation of IRF-3/IRF-7 which act as transcription factors that induce activation of the type I IFN promoter during viral infections. Involvement of different pathways in the induction of type I IFN is critically dependent on the virus species and cell type. Cell type-specific contributions of other sensors, including DEAD box helicases, might occur in some cases of infection. However, in hepatocytes, the control plasmid per se exhibited no IFN-inducing response, suggesting that the HBV replication is a critical step for IFN induction. Actually, no contribution of other sensors except RIG-I/MDA5 and TLR3 has been reported so far.

Using the murine hydrodynamic injection model, we found that mice deficient in IRF-3 and IRF-7 or IFNAR do not inhibit HBV replication as effectively as their WT counterparts and result in elevated HBV titers in mice sera and livers. These findings imply that type I IFN acting on IFNAR is indispensable for evoking anti-HBV protective responses although such a hypothesis is in disagreement with previous findings that HBV does not induce detectable changes in type I IFN expression during the early weeks of infection [34]. There are a few possibilities of how type I IFN is produced in mice receiving HBV template plasmid. One of them is that HBV could be recognized by pathways that do not link to MAVS or TICAM-1 and facilitate IFN production in the cytoplasm. For instance, STING-dependent signaling leads to type I IFN induction, and it has been shown that this can be MAVS and TICAM-1 independent. Notably, STING-dependent signaling is especially associated with DNA-mediated induction of type I IFN via IRF-3/IRF-7, and genomic DNA is an important part of HBV replication. It would be interesting to clarify such hypotheses using *Sting*$^{-/-}$ mice in the near future.

To elucidate the molecular pattern which triggers type I IFN induction, we transfected either HBV DNA or RNA into immortalized hepatocytes. To our surprise, we were unable to detect significant IFN-β induction with either HBV replicative DNA or HBV RNA. As we looked into the possible reasons to account for the lack of innate immune responses against HBV in hepatocytes, we found that the endogenous expression of STING in hepatocyte cell lines including HepG2 and immortalized mouse hepatocytes is extremely low compared to other cell lines like macrophages or dendritic cells, thus suggesting that STING-dependent signaling might play a crucial role in inducing type I IFN in response to HBV. The produced IFN in turn activates the IFNAR pathway. There are various cells populations in the liver that express IFNAR and therefore subsequently initiate a natural signaling cascade for amplification of IFN production via the Jak-STAT pathway.

Another possible way for HBV to induce IFN is via the HBV-stimulated nonparenchymal or resident myeloid cells. Even though there has been no report suggesting that HBV substantially infects pDCs, Isogawa et al. [5], demonstrated that freshly isolated CD11c^{+} cells of intrahepatic myeloid cells rather than the hepatocytes expressed TLRs including TLR2, 3, and 9. Therefore, resident myeloid cells might induce IFN to further prevent the spread of HBV by activating the IFNAR pathway in bystander cells or hepatocytes.

Although *Myd88*$^{-/-}$ mice receiving an HBV-DNA injection did not exhibit significantly high virus titers in the early phase unlike those observed in *Ifnar*$^{-/-}$ and *Irf-3*$^{-/-}$/*Irf-7*$^{-/-}$ mice, interestingly MyD88 is required for the intrahepatic clearance of the HBV replicative template. The fact that the transcriptional template persists in the absence of MyD88 suggests that MyD88 may play a pivotal role in intrahepatic HBV clearance in the mouse model. Notably, MyD88 is the adaptor molecule for TLR7 and 9 in pDCs [35, 36]. Deficiency of MyD88 in pDCs may result in failure to induce acquired immunity for HBV. Our findings show that HBV-specific antibodies are efficiently produced in WT, but not in *Myd88*$^{-/-}$ mice. In addition, the number of pDCs has been previously reported to be reduced in vivo during several systemic viral infections including HBV [37]. In one of the most recent reports, Lv et al. [38], showed that HBV-derived CpG induces potent IFN-α production by human pDCs, which may partially explain how pDCs interact with HBV in infection. However, the cause of weak participation in the early response of IFN induction in *Myd88*$^{-/-}$ mice remains to be determined.

Recombinant IFN-α is a standard treatment for chronic HBV patients. Nevertheless, direct treatment with IFN yields only about 30% improvement in HBV patients and little is known about why most chronic HBV patients do not respond to IFN therapy [39]. As demonstrated in our study, virus persistency can be independent of the type I

IFN-inducing system. This observation leads to the suggestion that type I IFN is indispensable for inducing antiviral molecules to control viral replication and spread before the onset of more specific and powerful adaptive immune responses. This appeared to be factual at least in our knockout mouse models as virus titers were highly elevated in *Ifnar*$^{-/-}$ mice in the initial days after injection. Conversely, type I IFN did not have any influential effects on clearance of the HBV template in the later stages. Such observations coincide with the latest study conducted in patients with chronic HBV infection by Tan et al. [40], in which IFN-α treatment was shown to modulate innate immune parameters in the patients, but without any detectable effect on HBV-specific adaptive immunity. The missing link between the induction of type I IFN and anti-HBV cellular effectors needs to be further investigated in mouse models, including the mechanism of MyD88 participation in activation of the cellular immune response during infection. Elucidating molecular mechanisms between innate pattern sensing and evoking cellular effectors may provide a reasonable explanation for the failure of IFN-treatment in HBV infection.

Collectively, our study validates the use of the hydrodynamic transfection method in mimicking acute HBV infection in mouse models and demonstrated the host-virus relationship during HBV infection in many aspects. Since HBV infectious models with immunologically well-defined laboratory animals do not exist, the result presented in this study herein provides an insight into the dispensability of RNA sensors for induction of IFN by HBV RNA and the complexity of innate and adaptive immunity during HBV clearance.

Acknowledgements

This work was supported in part by Grants-in-Aid from the Ministry of Education, Science, and Culture and the Ministry of Health, Labor, and Welfare of Japan, and the Yasuda Cancer Foundation (T.S.) and the Ono Foundation (T.S.). Financial support by a MEXT Grant-in-Project 'The Carcinogenic Spiral', 'The National Cancer Center Research and Development Fund (23-A-44)', and the Japan Initiative for Global Research Network on Infectious Diseases (J-GRID) are gratefully acknowledged. We are grateful to Drs. H. Shime, J. Kasamatsu, K. Funami, and M. Tatematsu in our laboratory for their fruitful discussions. We thank Dr. F.V. Chisari (Scripps Research Institute, La Jolla, Calif., USA) for providing us with HBV plasmid and sleeping beauty.

Disclosure Statement

The authors declare no financial or commercial conflict of interest.

References

1 Guidotti LG, Chisari FV: Immunobiology and pathogenesis of viral hepatitis. Annu Rev Pathol 2006;1:23–61.
2 Zuckerman JN, Zuckerman AJ: Current topics in hepatitis B. J Infect 2000;41:130–136.
3 Ganem D, Prince AM: Hepatitis B virus infection – natural history and clinical consequences. N Engl J Med 2004;350:1118–1129.
4 Seeger C, Mason WS: Hepatitis B virus biology. Microbiol Mol Biol Rev 2000;64:51–68.
5 Isogawa M, Robek MD, Furuichi Y, Chisari FV: Toll-like receptor signaling inhibits hepatitis B virus replication in vivo. J Virol 2005; 79:7269–7272.
6 Wu J, Lu M, Meng Z, Trippler M, Broering R, Szczeponek A, Krux F, Dittmer U, Roggendorf M, Gerken G, Schlaak JF: Toll-like receptor-mediated control of HBV replication by nonparenchymal liver cells in mice. Hepatology 2007;46:1769–1778.
7 Kawai T, Takahashi K, Sato S, Coban C, Kumar H, Kato H, Ishii KJ, Takeuchi O, Akira S: IPS-1, an adaptor triggering RIG-I- and Mda5-mediated type I interferon induction. Nat Immunol 2005;6:981–988.
8 Akira S, Uematsu S, Takeuchi O: Pathogen recognition and innate immunity. Cell 2006; 124:783–801.
9 Takeuchi O, Akira S: Innate immunity to virus infection. Immunol Rev 2009;227:75–86.
10 Oshiumi H, Matsumoto M, Funami K, Akazawa T, Seya T: TICAM-1, an adaptor molecule that participates in Toll-like receptor 3-mediated interferon-β induction. Nat Immunol 2003;4:161–167.
11 Ishikawa H, Ma Z, Barber GN: STING regulates intracellular DNA-mediated, type I interferon-dependent innate immunity. Nature 2009;461:788–792.
12 Cheng G: Double-stranded DNA and double-stranded RNA induce a common antiviral signaling pathway in human cells. Proc Natl Acad Sci USA 2007;104:9035–9040.
13 Ablasser A, Bauernfeind F, Hartmann G, Latz E, Fitzgerald KA, Hornung V: RIG-I-dependent sensing of poly(dA:dT) through the induction of an RNA polymerase III-transcribed RNA intermediate. Nat Immunol 2009;10:1065–1072.
14 Chiu YH, Macmillan JB, Chen ZJ: RNA polymerase III detects cytosolic DNA and induces type I interferons through the RIG-I pathway. Cell 2009;138:576–591.
15 Stetson DB, Medzhitov R: Type I interferons in host defense. Immunity 2006;25:373–381.
16 Kumar M, Jung SY, Hodgson AJ, Madden CR, Qin J, Slagle BL: Hepatitis B virus regulatory HBx protein binds to adaptor protein IPS-1 and inhibits the activation of beta interferon. J Virol 2011;85:987–995.
17 Wei C, Ni C, Song T, Liu Y, Yang X, Zheng Z, Jia Y, Yuan Y, Guan K, Xu Y, Cheng X, Zhang Y, Wang Y, Wen C, Wu Q, Shi W, Zhong H: The hepatitis B virus X protein disrupts innate immunity by down regulating mitochondrial antiviral signaling protein. J Immunol 2010; 185:1158–1168.
18 Yu S, Chen J, Wu M, Chen H, Kato N, Yuan Z: Hepatitis B virus polymerase inhibits RIG-I- and Toll-like receptor 3-mediated beta interferon induction in human hepatocytes through interference with interferon regulatory factor 3 activation and dampening of the interaction between TBK1/IKKepsilon and DDX3. J Gen Virol 2010;91:2080–2090.
19 Oshiumi H, Okamoto M, Fujii K, Kawanishi T, Matsumoto M, Koike S, Seya T: The TLR3/TICAM-1 pathway is mandatory for innate immune responses to poliovirus infection. J Immunol 2011;187:5320–5327.

20 Akazawa T, Ebihara T, Okuno M, Okuda Y, Shingai M, Tsujimura K, Takahashi T, Ikawa M, Okabe M, Inoue N, et al: Antitumor NK activation induced by the Toll-like receptor 3-TICAM-1 (TRIF) pathway in myeloid dendritic cells. Proc Natl Acad Sci USA 2007;104: 252–257.
21 Noguchi C, Ishino H, Tsuge M, Fujimoto Y, Imamura M, Takahashi S, Chayama K: G to A hypermutation of hepatitis B virus. Hepatology 2005;41:626–633.
22 Tian Y, Chen WL, Kuo CF, Ou JH: Viral-load-dependent effects of liver injury and regeneration on hepatitis B virus replication in mice. J Virol 2012;86:9599–9605.
23 Yang PL, Althage A, Chung J, Chisari FV: Hydrodynamic injection of viral DNA: a mouse model of acute hepatitis B virus infection. Proc Natl Acad Sci USA 2002;99:13825–13830.
24 Aly HH, Oshiumi H, Shime H, Matsumoto M, Wakita T, Shimotohno K, Seya T: Development of mouse hepatocyte lines permissive for hepatitis C virus (HCV). PLoS One 2011; 6:e21284.
25 Honda K, Taniguchi T: IRFs: master regulators of signalling by Toll-like receptors and cytosolic pattern-recognition receptors. Nat Rev Immunol 2006;6:644–658.
26 Wang X, Li Y, Mao A, Li C, Tien P: Hepatitis B virus X protein suppresses virus-triggered IRF3 activation and IFN-beta induction by disrupting the VISA-associated complex. Cell Mol Immunol 2010;7:341–348.
27 Kawai T, Akira S: Innate immune recognition of viral infection. Nat Immunol 2006;7:131–137.
28 Onomoto K, Yoneyama M, Fujita T: Regulation of antiviral innate immune responses by RIG-I family of RNA helicases. Curr Top Microbiol Immunol 2007;316:193–205.
29 Matsumoto M, Oshiumi H, Seya T: Antiviral responses induced by the TLR3 pathway. Rev Med Virol 2011, DOI: 10.1002/rmv.680.
30 Diebold SS: Recognition of viral single-stranded RNA by Toll-like receptors. Adv Drug Deliv Rev 2008;60:813–823.
31 Paludan SR, Bowie AG: Immune sensing of DNA. Immunity 2013;38:870–880.
32 Ishikawa H, Barber GN: The STING pathway and regulation of innate immune signaling in response to DNA pathogens. Cell Mol Life Sci 2011;68:1157–1165.
33 Suzuki T, Oshiumi H, Miyashita M, Aly HH, Matsumoto M, Seya T: Cell type-specific subcellular localization of phospho-TBK1 in response to cytoplasmic viral DNA. PLoS One 2013;8:e83639.
34 Bertoletti A, Gehring AJ: The immune response during hepatitis B virus infection. J Gen Virol 2006;87:1439–1449.
35 Hoshino K, Sasaki I, Sugiyama T, Yano T, Yamazaki C, Yasui T, Kikutani H, Kaisho T: Critical role of IkappaB Kinase alpha in TLR7/9-induced type I IFN production by conventional dendritic cells. J Immunol 2010; 184:3341–3345.
36 Hoshino K, Sugiyama T, Matsumoto M, Tanaka T, Saito M, Hemmi H, Ohara O, Akira S, Kaisho T: IkappaB kinase-alpha is critical for interferon-alpha production induced by Toll-like receptors 7 and 9. Nature 2006;440: 949–953.
37 Swiecki M, Wang Y, Vermi W, Gilfillan S, Schreiber RD, Colonna M: Type I interferon negatively controls plasmacytoid dendritic cell numbers in vivo. J Exp Med 2011;208: 2367–2374.
38 Lv S, Wang J, Dou S, Yang X, Ni X, Sun R, Tian Z, Wei H: Nanoparticles encapsulating HBV-CpG induce therapeutic immunity against hepatitis B virus infection. Hepatology 2014;59:385–394.
39 Ter Borg MJ, Hansen BE, Bigot G, Haagmans BL, Janssen HL: ALT and viral load decline during PEG-IFN alpha-2b treatment for HBeAg-positive chronic hepatitis B. J Clin Virol 2008;42:160–164.
40 Tan AT, Hoang LT, Chin D, Rasmussen E, Lopatin U, Hart S, Bitter H, Chu T, Gruenbaum L, Ravindran P, Zhong H, Gane E, Lim SG, Chow WC, Chen PJ, Petric R, Bertoletti A, Hibberd ML: Reduction of HBV replication prolongs the early immunological response to IFNα therapy. J Hepatol 2014;60: 54–61.

Biochemical and Biophysical Research Communications xxx (2015) 1–6

Contents lists available at ScienceDirect

Biochemical and Biophysical Research Communications

journal homepage: www.elsevier.com/locate/ybbrc

Pam2 lipopeptides systemically increase myeloid-derived suppressor cells through TLR2 signaling

Akira Maruyama [1], Hiroaki Shime[*, 1], Yohei Takeda, Masahiro Azuma, Misako Matsumoto, Tsukasa Seya[*]

Department of Microbiology and Immunology, Hokkaido University Graduate School of Medicine, Kita 15, Nishi 7, Kita-ku, Sapporo 060-8638, Japan

ARTICLE INFO

Article history:
Received 24 December 2014
Available online xxx

Keywords:
Myeloid-derive suppressor cells (MDSCs)
Pam2 lipopeptides
Toll-like receptor 2
Immunosuppression
Antitumor immunotherapy

ABSTRACT

Myeloid-derived suppressor cells (MDSCs) are immature myeloid cells that exhibit potent immunosuppressive activity. They are increased in tumor-bearing hosts and contribute to tumor development. Toll-like receptors (TLRs) on MDSCs may modulate the tumor-supporting properties of MDSCs through pattern-recognition. Pam2 lipopeptides represented by Pam2CSK4 serve as a TLR2 agonist to exert antitumor function by dendritic cell (DC)-priming that leads to NK cell activation and cytotoxic T cell proliferation. On the other hand, TLR2 enhances tumor cell progression/invasion by activating tumor-infiltrating macrophages. How MDSCs respond to TLR2 agonists has not yet been determined. In this study, we found intravenous administration of Pam2CSK4 systemically up-regulated the frequency of MDSCs in EG7 tumor-bearing mice. The frequency of tumor-infiltrating MDSCs was accordingly increased in response to Pam2CSK4. MDSCs were not increased by Pam2CSK4 stimuli in TLR2 knockout (KO) mice. Adoptive transfer experiments using CFSE-labeled MDSCs revealed that the TLR2-positive MDSCs survived long in tumor-bearing mice in response to Pam2CSK4 treatment. Since the increased MDSC population sustained immune-suppressive properties, our study suggests that Pam2CSK4-triggered TLR2 activation enhances the MDSC potential and suppress antitumor immune response in tumor microenvironment.

1. Introduction

TLR2 signaling pathway plays a critical role in induction of protective immunity against infection [1,2]. TLR2 enhances dendritic cell/macrophage functions that cause host defense, but exerts a controversial effect on cancer development [2]. Recent reports demonstrated that treatment with purified TLR2 ligands such as Pam2CSK4, Pam3CSK4, MALP2 or related synthetic compounds inhibited tumor growth in mice tumor implant models [3,4]. Pam2 lipopeptides trigger activation of TLR2 in combination with TLR6 or TLR1 in conventional DCs, which leads to maturation of the DCs through the MyD88-dependent signaling pathway, resulting in NK cell activation and CTL proliferation [5–7].

In tumor-bearing mice with systemic exposing to TLR2 agonists, however, an opposite effect was reported: TLR2 signal-induced inflammation may contribute to tumor progression. TLR2 is also expressed on immune cells with regulatory properties that include tumor-associated macrophages (TAMs), myeloid-derived suppressor cells (MDSCs) as well as tumor cells [8–10]. Host cell-derived endogenous TLR2 ligand, such as versican, a chondroitin sulfate proteoglycan derived from cancer cells, stimulates macrophages to produce TNF-α, which enhances lung metastasis of cancer cells [11]. Furthermore, Pam2CSK4 primes DC activation to induce expansion of $Foxp3^+CD25^+CD4^+$ regulatory T cells (Treg) and cause immune tolerance against cancer [12,13]. These reports suggest that TLR2 signaling may modulate the myeloid cell function, which promotes growth, invasion, or metastasis of tumor cells. There might be cell type-to-cell type difference in TLR2 response to its ligands, which critically determines their mode for regulation against tumor progression or survival.

MDSCs are heterogenous populations of immature myeloid cells that have immunosuppressive activity. MDSCs are expanded in

Abbreviations: CFSE, carboxyfluorescein succinimidyl ester; CTL, cytotoxic T lymphocyte; DAMP, damage-associated molecular pattern; DC, dendritic cell; MALP-2, macrophage activating lipopeptide-2; NK, natural killer; Pam2, 16 S-[2,3-bis(palmitoyl)propyl]cysteine; TLR, toll-like receptor.

* Corresponding authors. Fax: +81 11 706 7866.
E-mail addresses: shime@med.hokudai.ac.jp (H. Shime), seya-tu@pop.med.hokudai.ac.jp (T. Seya).

[1] The first two authors were equally contributed.

http://dx.doi.org/10.1016/j.bbrc.2015.01.011
0006-291X/

tumor-bearing mice and patients with cancer such as colon cancer, bladder cancer, lung cancer, and ovarian cancer. They impede the efficacy of cancer immunotherapy [14]. Depletion of MDSCs augments anti-tumor activity of host immune cells by restoring effector cell function [15]. Mouse MDSCs are characterized by the markers of $CD11b^{+}Gr1^{+}$. MDSCs subvert anti-tumor immunity by suppression of DC maturation, T cell proliferation and NK cell activation, and by induction of immunosuppressive M2 macrophage and Tregs [14,16,17]. MDSCs consist of $Ly6C^{high}Ly6G^{-}CD11b^{+}$ monocytic MDSCs (M-MDSCs) and $Ly6C^{low}Ly6G^{+}CD11b^{+}$ granulocytic MDSCs (G-MDSCs). Both subsets show distinct features and exert immunosuppressive activity by different mechanisms [18]. Inflammation-associated molecules induce accumulation of MDSCs and enhance immunosuppressive activity in local environment. Recent reports demonstrated that TLR signaling regulated tumor growth by modifying MDSC function [19]. MDSCs express TLRs, through which TLR ligands modify their accumulation, differentiation and function [20]. Tumor cell-derived exosomes containing Hsp72 induce expansion and suppressive activity of MDSCs through the TLR2-IL-6-STAT3 axis [9]. The S100A8/A9 complex produced in tumor regulates accumulation and suppressive activity of MDSCs through the TLR4 signaling pathway [21,22]. On the other hand, TLR9 and TLR3 ligands such as CpG ODN and poly I:C, respectively, are demonstrated to modify MDSC function directly or indirectly. Those functionally modified MDSCs exhibit loss of immunosuppressive activity against T cell function as well as act as the accessory cells for NK cell activation [23–25]. In this context, what happens in MDSCs when TLR2 agonist is exogenously administered to tumor-bearing mice remains poorly understood.

In this study, we revealed that Pam2CSK4 induces accumulation of MDSCs in spleen and tumor in tumor-bearing hosts. Pam2CSK4 can support long survival of MDSCs through the TLR2 signaling pathway.

2. Materials and methods

2.1. Mice and cells

C57BL/6J (B6 WT) female mice were obtained from CLEA Japan Inc. (Tokyo, Japan). $TLR2^{-/-}$ mice were provided by Dr. Shizuo Akira (Osaka University, Osaka, Japan). C57BL6-Tg (CAG-EGFP) mice (EGFP transgenic mice) were provided by Dr. Masaru Okabe (Osaka University). The mice were maintained in the Hokkaido University Animal Facility (Sapporo, Jappan). *Mice of 8- to 12-weeks of age* were used in all experiments that were performed according to animal experimental ethics committee guidelines of Hokkaido University. EG7 cells were purchased from ATCC and cultured in RPMI1640/10% FCS/55 μM 2-ME/1 mM sodium pyruvate/penicillin/streptomycin. B16D8 cells were established in our laboratory and cultured in RPMI1640/10% FCS/penicillin/streptomycin [26].

2.2. Reagents and antibodies

FITC-conjugated anti-CD45 (30-F11), Alexa-700 or APC-conjugated anti-CD45.2 (104), Alexa 700, FITC or PE-conjugated anti-CD11b (M1/70), biotinylated, APC-conjugated anti-Gr-1 (RB6-8C5), purified anti-CD16/CD32 (2.4G2), and isotype antibodies were obtained from Biolegend (San Diego, CA, USA). 2,3-bis (palmitoyl) propyl CSKKKK (Pam2CSK4) was synthesized by Biologica Co. Ltd (Nagoya, Japan). To rule out LPS contamination, we treated Pam2CSK4 with 200 μg/ml of polymixin B for 30 min at 37 °C before use.

2.3. Tumor models

Mice were shaved at the back and injected subcutaneously (s.c.) with EG7 cells (1×10^6) or B16D8 (6×10^5) suspended in 200 μl PBS(−). When tumor grew, tumor size was measured using a caliper. In some experiments, Pam2CSK4 was i.p. injected into tumor-bearing mice. Tumor volume was calculated using the following formula: tumor volume (cm^3) = (long diameter) × (short diameter)^2 × 0.4. Pam2CSK4 was injected intravenously (i.v.) as indicated.

2.4. Isolation of cells

Tumor-infiltrating myeloid cells were defined by gating in FACS-sorting as previously described [25,27]. $CD11b^{+}Gr1^{+}$ MDSCs were separated with anti-Gr-1 biotinylated antibody and streptavidin microbeads (Miltenyi Biotech) from spleen cell suspensions of EG7 tumor-bearing mice. The purity of isolated cells was more than 90% as assessed by flow cytometory. Almost 100% of $Gr1^{+}$ cells were $CD11b^{+}$.

2.5. Flow cytometric analysis

Cells prepared from mouse spleen, blood or tumor were blocked with anti-CD16/32 antibody and stained with fluorescent antibodies. Samples were analyzed with the FACS Calibur instrument or the FACS Aria II instrument (BD Bioscience) and data analysis was performed by the Flow Jo software (Tree Star, USA).

2.6. Cell proliferation assay

T cell proliferation was measured by changes in fluorescence intensity using CFSE. OT-I splenocytes were labeled with 1 μM CFSE for 10 min and cultured with CD11b + Gr1 + MDSC in the presence of 50 nM SL8 peptide ($OVA_{257-264}$) and/or 100 nM Pam2CSK4. After 3 days, cells were harvested, stained with APC-anti-CD8α and PE-anti-TCR vβ 5.1, 5.2 or Alexa 700-anti-CD3ε, and CFSE signal of the gated lymphocytes was analyzed with a FACS Calibur instrument or FACS Aria II instrument. The extent of cell proliferation was quantified by Flow Jo software.

2.7. Adoptive transfer

EG7 tumor-bearing mice were injected i.v. with 5×10^6 CFSE-labeled MDSCs, and then injected i.v. with 50 nmol Pam2CSK4. After 24 h, spleen cells were blocked with anti-CD16/32 antibody and stained with fluorescent antibodies. Samples were measured by flow cytometry using the FACS Aria II. Data analysis was performed using the Flow Jo software.

2.8. Statistics

If not otherwise stated, data were expressed as arithmetic means ± SD, and statistical analyses were made by 2-tailed Student's t test. $p < 0.05$ was considered statistically significant.

3. Results

3.1. Expansion of TLR2-expressing MDSCs in EG7 tumor-bearing mice

We examined TLR2 expression on MDSCs in C57BL6/J mice subcutaneously (s.c.) implanted with EG7 lymphoma cells. 21 days after tumor inoculation when tumor volumes reached 4–8 cm^3, spleen cells of the tumor-bearing mice were analyzed by flow

Please cite this article in press as: A. Maruyama, et al., Pam2 lipopeptides systemically increase myeloid-derived suppressor cells through TLR2 signaling, Biochemical and Biophysical Research Communications (2015), http://dx.doi.org/10.1016/j.bbrc.2015.01.011

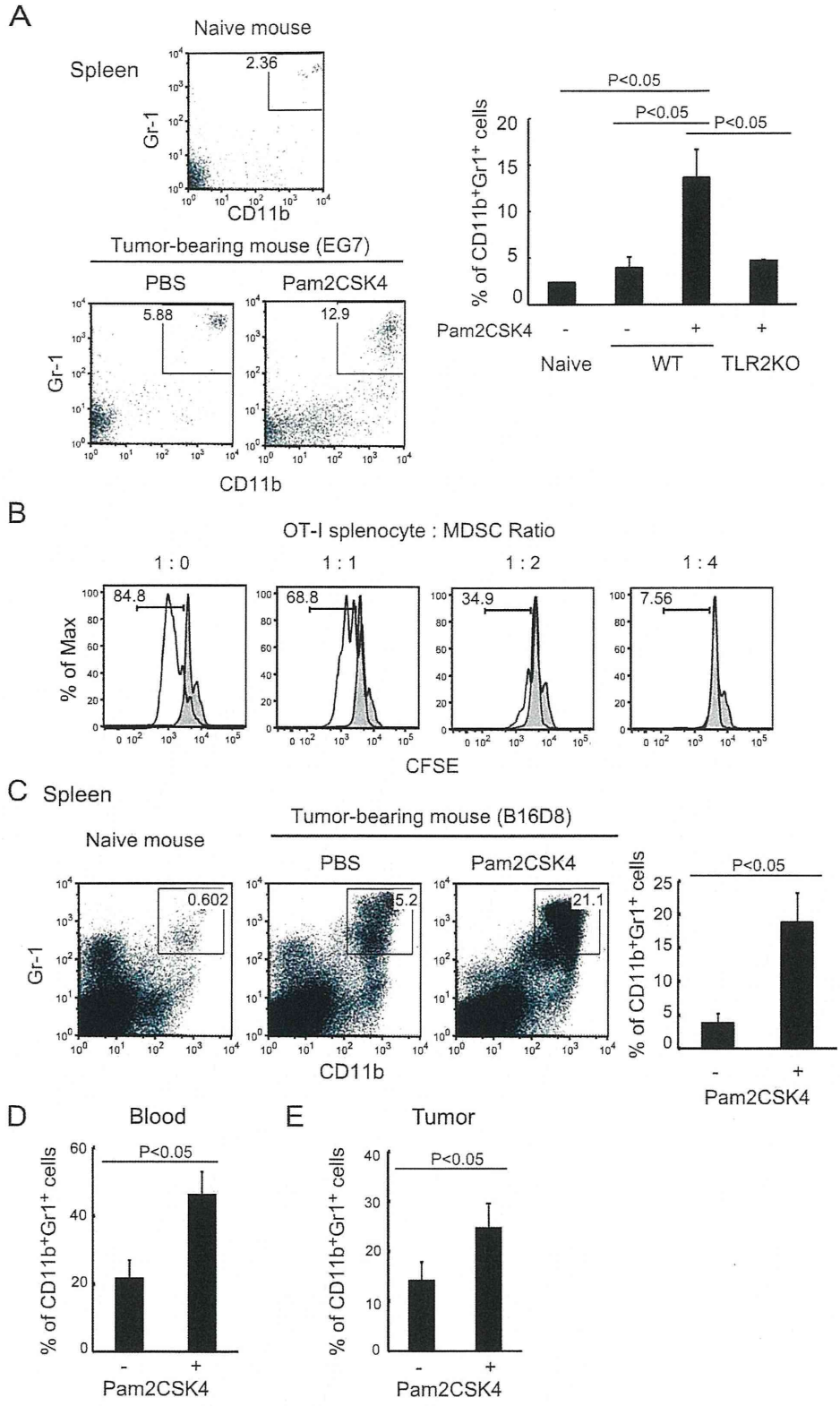

Fig. 1. Pam2CSK4 treatment induces accumulation of $CD11b^+Gr1^+$ MDSCs in tumor-bearing mice through TLR2 signaling. EG7 lymphoma cells (1×10^6) were implanted s.c. into B6 WT mice (A, B, and D), TLR2 KO mice (A) or EGFP transgenic mice (E) as described in materials and methods. B16D8 cells (6×10^5) were implanted s.c. into B6 WT mice (C). When tumor size was reached between 1 and 2.5 cm^3 (23–28 days after inoculation), mice were injected i.v. with PBS or 50 nmol Pam2CSK4. After 48 h, spleens (A and C), peripheral blood (D), and tumors (E) were isolated and the frequency of $CD11b^+Gr1^+$ cells in $CD45^+$ cells (A, C, and D) or in GFP^+CD45^+ cells (E) was determined by flow cytometory. Data shown in the graph represent mean ± SD. n = 3. Numbers in the graph represent the percentage of gated cells. In (B), $CD11b^+Gr1^+$ cells were isolated from EG7 tumor-bearing mice and analyzed suppressive activity on OT-I T cell proliferation as described in materials and methods. The CFSE histograms are gated for $CD8\alpha^+$TCR vβ 5.1, 5.2^+ cells. Open or closed histograms represent the cells cultured in the presence or absence of SL8 peptides, respectively. The numbers indicate the percentage of proliferated cells in open histograms.

Please cite this article in press as: A. Maruyama, et al., Pam2 lipopeptides systemically increase myeloid-derived suppressor cells through TLR2 signaling, Biochemical and Biophysical Research Communications (2015), http://dx.doi.org/10.1016/j.bbrc.2015.01.011

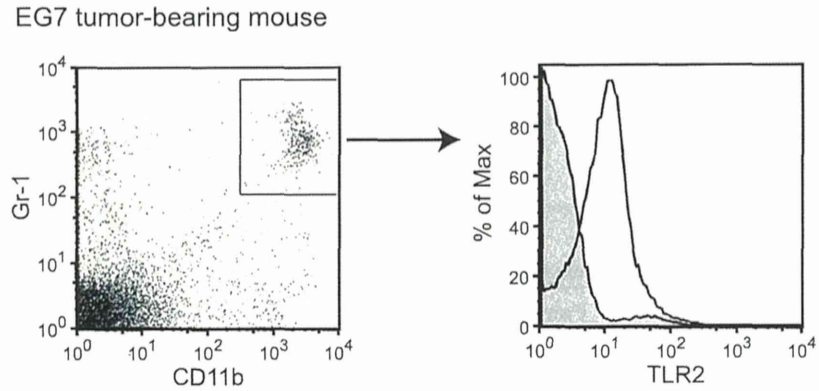

Fig. 2. CD11b$^+$Gr1$^+$ MDSCs express TLR2 on their surface. TLR2 expression level on CD11b$^+$Gr1$^+$ cells in spleen of EG7 tumor-bearing mice (21 days after tumor challenge) was analyzed by flow cytometory. The open histogram represents staining with anti-TLR2 antibody and the shaded histogram represent staining with isotype control antibody.

cytometory. The frequency of CD11b$^+$Gr1$^+$ cells in spleens was significantly increased in EG7 tumor-bearing mice compared with tumor-free mice (Fig. 1A). CD11b$^+$Gr1$^+$ cells harvested from tumor-bearing mice treated with Pam2CSK4 suppressed antigen-dependent T cell proliferation in a dose-dependent manner when cocultured with OT-I splenocytes, demonstrating that this population had MDSC-like activity (Fig. 1B). We found that TLR2 was highly expressed in CD11b$^+$Gr1$^+$ MDSCs in spleen judged by flow cytometoric analysis (Fig. 2). Thus, our results indicate that TLR2-expressing MDSCs are expanded in EG7 tumor-bearing mice.

3.2. *Pam2CSK4 treatment induces accumulation of MDSCs in tumor-bearing mice through TLR2-dependent mechanism*

To examine whether TLR2 activation by Pam2CSK4 affects accumulation of MDSCs *in vivo*, we analyzed the proportion of CD11b$^+$Gr1$^+$ cells in tumor-bearing mice after Pam2CSK4 i.v. injection. We measured the percentage of CD11b$^+$Gr1$^+$ cells in spleens in EG7 tumor-bearing mice 48 h after Pam2CSK4 administration. Although the proportion of CD45$^+$ cells in spleen was not altered (85 ± 6.07% of PBS-treated mice vs 87.3 ± 7.11% of Pam2CSK4-treated mice), Pam2CSK4 administration significantly increased the percentage of CD11b$^+$Gr1$^+$ cells in CD45$^+$ cells of spleens in EG7 tumor-bearing mice (Fig. 1A). CD11b$^+$Gr1$^+$ cells harvested from the spleens of Pam2CSK4-treated tumor-bearing mice suppressed T cell proliferation in a dose-dependent manner when the cells were co-cultured with OT-1 splenocytes, demonstrating that this myeloid population had MDSC-like activity (Fig. 1B). Similar results were obtained with spleen CD11b$^+$Gr1$^+$ cells in B16-implanted mice (Fig. 1C, data not shown). The increased percentage of CD11b$^+$Gr1$^+$ cells was not observed after Pam2CSK4 treatment in TLR2$^{-/-}$ mice implanted with EG7 tumor (Fig. 1A). Pam2CSK4 facilitated systemic increases of CD11b$^+$Gr1$^+$ MDSCs: incremental MDSCs were confirmed in spleens, circulating blood and tumors. The percentage of CD11b$^+$Gr1$^+$ cells in peripheral blood was increased in peripheral blood in response to Pam2CSK4 treatment (Fig. 1D). To examine whether MDSCs accumulate in tumor, we used EGFP transgenic mice to distinguish host-derived CD45$^+$ cells from EG7 cells which also express CD45. Although the proportion of GFP-positive cells in tumor was barely changed, the percentage of CD11b$^+$Gr1$^+$ cells in GFP-positive cells was increased 48 h after Pam2CSK4 treatment (Fig. 1E). Thus, these results suggest that TLR2 activation induced by Pam2CSK4 leads to systemic accumulation of MDSCs rather than organ-specific recruitment of MDSCs in tumor-bearing mice.

3.3. *Pam2CSK4 treatment supports survival of MDSCs in tumor-bearing mice*

MDSCs are a short-lived cell population which shows rapid turnover in tumor-bearing mice [28]. We examined whether Pam2CSK4 prolonged survival of MDSCs *in vivo*. MDSCs were

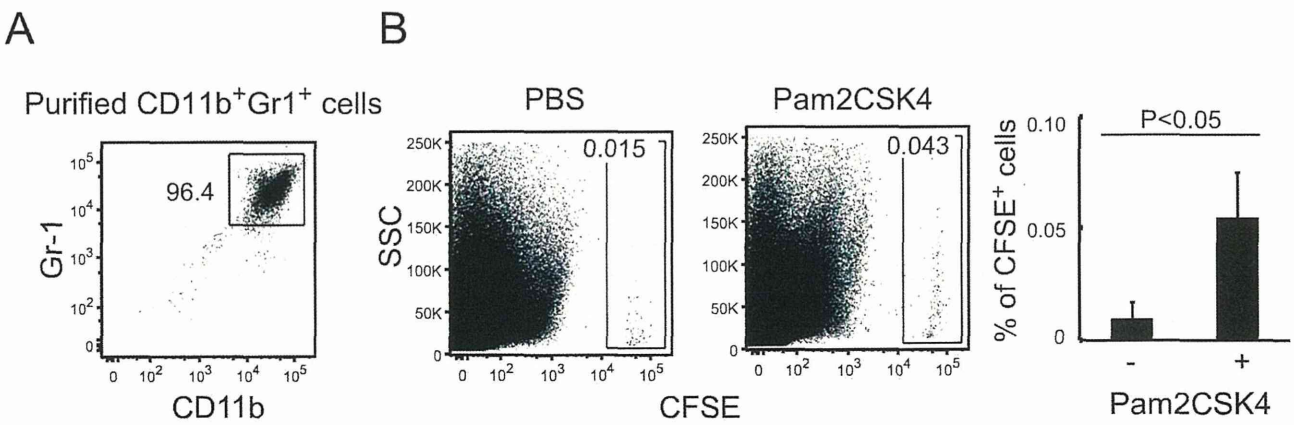

Fig. 3. Pam2CSK4 supports survival of adoptive transferred CD11b$^+$Gr1$^+$ cells in tumor-bearing mice. CD11b$^+$Gr1$^+$ cells (A) isolated from spleens of EG7 tumor-bearing mice were labeled with CFSE and adoptively transferred into EG7 tumor-bearing mice. The mice were injected i.v. with PBS or 50 nmol Pam2CSK4. After 24 h, spleen cells were analyzed by flow cytometory (B). The frequency of CFSE-positive cells was determined. The numbers indicate the percentage of CFSE-positive cells in CD45$^+$-gated splenocytes.

Please cite this article in press as: A. Maruyama, et al., Pam2 lipopeptides systemically increase myeloid-derived suppressor cells through TLR2 signaling, Biochemical and Biophysical Research Communications (2015), http://dx.doi.org/10.1016/j.bbrc.2015.01.011

isolated from the spleen of tumor-bearing mice and labeled with CFSE, and then adoptively transferred into EG7 tumor-bearing mice. Treatment with poly I: C increased percentage of remaining CFSE-positive cells in CD45-positive splenocytes of EG7 tumor-bearing mice (Fig. 3A and B). Thus, our results suggest that Pam2CSK4 may support survival of MDSCs in tumor-bearing mice through the TLR2-dependent signaling pathway. CFSE-positive cells barely proliferated in the bone marrow within our setting (data not shown).

4. Discussion

Although TLR2 ligands can induce tumor regression by inducing anti-tumor immune responses mediated by DCs, cytotoxic T lymphocytes and NK cells, their effects on immunosuppressive cells including MDSCs have not been fully investigated. The purpose of this study was to determine the role of TLR2 signaling on accumulation of immunosuppressive MDSCs in tumor-bearing hosts. Our findings revealed that Pam2CSK4-induced TLR2 signaling enhances systemic expansion of MDSCs *in vivo*. Since MDSCs have strong immunosuppressive activity against anti-tumor immunity, our results suggest that treatment with TLR2 ligands may lead to augmentation of immunosuppression in tumor-bearing hosts.

MDSCs consist of two major subsets of M-MDSCs and G-MDSCs, both of which express TLR2. They show distinct morphology and differential mechanisms for immunosuppressive profiles. G-CSF, GM-CSF, and M-CSF are known as key growth factors for the regulation of survival, proliferation, and differentiation of MDSC subsets [29,30]. G-CSF or GM-CSF supports the survival of G-MDSCs in vitro [31]. TLR2 stimulation induces the production of these growth factors [32]. Intracellular signaling triggered by these growth factors contribute to the proliferation and survival of immature myeloid cells and prevent their differentiation to mature cells, resulting in accumulation of MDSCs. However, second signal induced by prolinflamamtory cytokines or TLR ligands are required to acquire immunosuppressive function [29]. TLR2 signal also induces the production of proinflammatory cytokines such as IL-6 and TNF-α by myeloid cells. A previous report demonstrated that TLR2 signal-induced IL-6 production was responsible for the development and survival of MDSCs through STAT3 activation [9]. TNF receptor signaling promotes the survival and accumulation of MDSCs [33]. S100A8/A9, which are produced by TLR2 signal activation, regulates the accumulation of MDSCs [34]. Thus, TLR2 signal may support survival and differentiation of MDSCs by inducing production of these cytokines in inflammatory milieu. TLR2 activation also induces proliferation of cancer cells by up-regulating the expression of numerous cell cycle progression and cell survival/anti-apoptosis genes [10], suggesting that TLR signal may directly induce survival or proliferation of MDSCs. Further analysis is required to identify the mechanisms that support MDSC accumulation by activating TLR2 signal.

MDSCs have strong immunosuppressive activity against CTLs, NK cells and DCs by producing immunosuppressive factors including arginase, TGF-β, reactive oxygen species (ROS), reactive nitrogen species (RNS), and IL-10. MDSCs also induce Tregs by producing arginase and/or IL-10 [14]. It remains unclear whether Pam2CSK4 influences immunosuppressive functions of MDSCs. In fact, Pam2CSK4 induces IL-10 and ROS production by DCs and macrophages through TLR2 signaling [35]. Therefore, Pam2CSK4 may not only support the survival but also regulate the immunosuppressive activity of MDSCs because the production of these molecules is tightly regulated by TLR2 signaling.

The regulatory mechanism of MDSC accumulation seems to be important for development of the effective therapeutic strategies to control these cells. MDSCs are produced in response to tumor-derived factors such as cytokines, chemokines, DAMPs, or microenvironmental factors such as hypoxia. Some of those are also provided by immune cells activated by endogenous ligand-induced TLR signaling. Our results suggest that MDSCs accumulate in tumor-bearing hosts in response to exogenously added TLR2 ligands. Adjuvant immunotherapy for cancer using TLR2 ligands has been proposed and some clinical trials are in progress [36]. Our results, however, unveiled the negative effects of TLR2 ligands on tumor immunity in terms of MDSC frequencies. Several reports demonstrated that the frequency of MDSCs is correlated with tumor size in several mouse models. MDSCs are frequently observed in patients with advanced cancer. Thus, TLR2 signal-induced accumulation of MDSCs may be critical for determining of success in immunotherapy against advanced cancer. The quality and properties of MDSCs have to be changed in TLR2 adjuvant therapy as in previous reports [25,27]. This point needs to be taken into consideration prior to the development of antitumor immunotherapy for cancer.

Conflict of interest statement

The authors have no conflict of interest.

Acknowledgments

This work was supported in part by Grants-in-Aid from the Ministry of Education, Science, and Culture (MEXT), "the Carcinogenic Spiral" a MEXT Grant-in-Project, the Ministry of Health, Labor, and Welfare of Japan, the Takeda Foundation, and the Kato Memorial Bioscience Foundation.

References

[1] T. Kawai, S. Akira, The role of pattern-recognition receptors in innate immunity: update on toll-like receptors, Nat. Immunol. 11 (2010) 373–384, http://dx.doi.org/10.1038/ni.1863.
[2] A. Mantovani, P. Allavena, A. Sica, F. Balkwill, Cancer-related inflammation, Nature 454 (2008) 436–444, http://dx.doi.org/10.1038/nature07205.
[3] T. Akazawa, H. Masuda, Y. Saeki, M. Matsumoto, K. Takeda, K. Tsujimura, et al., Adjuvant-mediated tumor regression and tumor-specific cytotoxic response are impaired in MyD88-deficient mice, Cancer Res. 64 (2004) 757–764.
[4] T. Seya, H. Shime, T. Ebihara, H. Oshiumi, M. Matsumoto, Pattern recognition receptors of innate immunity and their application to tumor immunotherapy, Cancer Sci. 101 (2010) 313–320, http://dx.doi.org/10.1111/j.1349-7006.2009.01442.x.
[5] M. Azuma, R. Sawahata, Y. Akao, T. Ebihara, S. Yamazaki, M. Matsumoto, et al., The peptide sequence of diacyl lipopeptides determines dendritic cell TLR2-mediated NK activation, PLoS ONE 5 (2010), http://dx.doi.org/10.1371/journal.pone.0012550.
[6] R. Sawahata, H. Shime, S. Yamazaki, N. Inoue, T. Akazawa, Y. Fujimoto, et al., Failure of mycoplasma lipoprotein MALP-2 to induce NK cell activation through dendritic cell TLR2, Microbes Infect. 13 (2011) 350–358, http://dx.doi.org/10.1016/j.micinf.2010.12.003.
[7] K.-Y. Shen, Y.-C. Song, I.-H. Chen, C.-H. Leng, H.-W. Chen, H.-J. Li, et al., Molecular mechanisms of TLR2-mediated antigen cross-presentation in dendritic cells, J. Immunol. 192 (2014) 4233–4241, http://dx.doi.org/10.4049/jimmunol.1302850.
[8] T.A. Wynn, A. Chawla, J.W. Pollard, Macrophage biology in development, homeostasis and disease, Nature 496 (2013) 445–455, http://dx.doi.org/10.1038/nature12034.
[9] F. Chalmin, S. Ladoire, G. Mignot, J. Vincent, M. Bruchard, J.-P. Remy-Martin, et al., Membrane-associated Hsp72 from tumor-derived exosomes mediates STAT3-dependent immunosuppressive function of mouse and human myeloid-derived suppressor cells, J. Clin. Invest 120 (2010) 457–471, http://dx.doi.org/10.1172/JCI40483.
[10] H. Tye, C.L. Kennedy, M. Najdovska, L. McLeod, W. McCormack, N. Hughes, et al., STAT3-driven upregulation of TLR2 promotes gastric tumorigenesis independent of tumor inflammation, Cancer Cell. 22 (2012) 466–478, http://dx.doi.org/10.1016/j.ccr.2012.08.010.
[11] S. Kim, H. Takahashi, W.-W. Lin, P. Descargues, S. Grivennikov, Y. Kim, et al., Carcinoma-produced factors activate myeloid cells through TLR2 to stimulate metastasis, Nature 457 (2009) 102–106, http://dx.doi.org/10.1038/nature07623.
[12] R.P.M. Sutmuller, M.H.M.G.M. den Brok, M. Kramer, E.J. Bennink, L.W.J. Toonen, B.-J. Kullberg, et al., Toll-like receptor 2 controls expansion and

function of regulatory T cells, J. Clin. Invest 116 (2006) 485–494, http://dx.doi.org/10.1172/JCI25439.
[13] S. Yamazaki, K. Okada, A. Maruyama, M. Matsumoto, H. Yagita, T. Seya, TLR2-dependent induction of IL-10 and Foxp3+ CD25+ CD4+ regulatory T cells prevents effective anti-tumor immunity induced by Pam2 lipopeptides in vivo, PLoS ONE 6 (2011) e18833, http://dx.doi.org/10.1371/journal.pone.0018833.
[14] D.I. Gabrilovich, S. Ostrand-Rosenberg, V. Bronte, Coordinated regulation of myeloid cells by tumours, Nat. Rev. Immunol. 12 (2012) 253–268, http://dx.doi.org/10.1038/nri3175.
[15] M.K. Srivastava, L. Zhu, M. Harris-White, U. Kar, U.K. Kar, M. Huang, et al., Myeloid suppressor cell depletion augments antitumor activity in lung cancer, PLoS ONE 7 (2012) e40677, http://dx.doi.org/10.1371/journal.pone.0040677.
[16] B. Huang, P.-Y. Pan, Q. Li, A.I. Sato, D.E. Levy, J. Bromberg, et al., Gr-1+CD115+ immature myeloid suppressor cells mediate the development of tumor-induced T regulatory cells and T-cell anergy in tumor-bearing host, Cancer Res. 66 (2006) 1123–1131, http://dx.doi.org/10.1158/0008-5472.CAN-05-1299.
[17] P. Serafini, S. Mgebroff, K. Noonan, I. Borrello, Myeloid-derived suppressor cells promote cross-tolerance in B-cell lymphoma by expanding regulatory T cells, Cancer Res. 68 (2008) 5439–5449, http://dx.doi.org/10.1158/0008-5472.CAN-07-6621.
[18] J.-I. Youn, S. Nagaraj, M. Collazo, D.I. Gabrilovich, Subsets of myeloid-derived suppressor cells in tumor-bearing mice, J. Immunol. 181 (2008) 5791–5802.
[19] S.K. Bunt, V.K. Clements, E.M. Hanson, P. Sinha, S. Ostrand-Rosenberg, Inflammation enhances myeloid-derived suppressor cell cross-talk by signaling through toll-like receptor 4, J. Leukoc. Biol. 85 (2009) 996–1004, http://dx.doi.org/10.1189/jlb.0708446.
[20] S. Ostrand-Rosenberg, P. Sinha, Myeloid-derived suppressor cells: linking inflammation and cancer, J. Immunol. 182 (2009) 4499–4506, http://dx.doi.org/10.4049/jimmunol.0802740.
[21] P. Sinha, C. Okoro, D. Foell, H.H. Freeze, S. Ostrand-Rosenberg, G. Srikrishna, Proinflammatory S100 proteins regulate the accumulation of myeloid-derived suppressor cells, J. Immunol. 181 (2008) 4666–4675, http://dx.doi.org/10.4049/jimmunol.181.7.4666.
[22] P. Cheng, C.A. Corzo, N. Luetteke, B. Yu, S. Nagaraj, M.M. Bui, et al., Inhibition of dendritic cell differentiation and accumulation of myeloid-derived suppressor cells in cancer is regulated by S100A9 protein, J. Exp. Med. 205 (2008) 2235–2249, http://dx.doi.org/10.1084/jem.20080132.
[23] C. Zoglmeier, H. Bauer, D. Nörenberg, G. Wedekind, P. Bittner, N. Sandholzer, et al., CpG blocks immunosuppression by myeloid-derived suppressor cells in tumor-bearing mice, Clin. Cancer Res. 17 (2011) 1765–1775, http://dx.doi.org/10.1158/1078-0432.CCR-10-2672.
[24] Y. Shirota, H. Shirota, D.M. Klinman, Intratumoral injection of CpG oligonucleotides induces the differentiation and reduces the immunosuppressive activity of myeloid-derived suppressor cells, J. Immunol. 188 (2012) 1592–1599, http://dx.doi.org/10.4049/jimmunol.1101304.
[25] H. Shime, A. Kojima, A. Maruyama, Y. Saito, H. Oshiumi, M. Matsumoto, et al., Myeloid-derived suppressor cells confer tumor-suppressive functions on natural killer cells via polyinosinic: polycytidylic acid treatment in mouse tumor models, J. Innate Immun. 6 (2014) 293–305, http://dx.doi.org/10.1159/000355126.
[26] T. Akazawa, T. Ebihara, M. Okuno, Y. Okuda, M. Shingai, K. Tsujimura, et al., Antitumor NK activation induced by the toll-like receptor 3-TICAM-1 (TRIF) pathway in myeloid dendritic cells, Proc. Natl. Acad. Sci. U. S. A. 104 (2007) 252–257, http://dx.doi.org/10.1073/pnas.0605978104.
[27] H. Shime, M. Matsumoto, H. Oshiumi, S. Tanaka, A. Nakane, Y. Iwakura, et al., Toll-like receptor 3 signaling converts tumor-supporting myeloid cells to tumoricidal effectors, Proc. Natl. Acad. Sci. U. S. A. 109 (2012) 2066–2071, http://dx.doi.org/10.1073/pnas.1113099109.
[28] Y. Sawanobori, S. Ueha, M. Kurachi, T. Shimaoka, J.E. Talmadge, J. Abe, et al., Chemokine-mediated rapid turnover of myeloid-derived suppressor cells in tumor-bearing mice, Blood 111 (2008) 5457–5466, http://dx.doi.org/10.1182/blood-2008-01.
[29] T. Condamine, D.I. Gabrilovich, Molecular mechanisms regulating myeloid-derived suppressor cell differentiation and function, Trends Immunol. 32 (2011) 19–25, http://dx.doi.org/10.1016/j.it.2010.10.002.
[30] N. Sonda, M. Chioda, S. Zilio, F. Simonato, V. Bronte, Transcription factors in myeloid-derived suppressor cell recruitment and function, Curr. Opin. Immunol. 23 (2011) 279–285, http://dx.doi.org/10.1016/j.coi.2010.12.006.
[31] J.I. Youn, M. Collazo, I.N. Shalova, S.K. Biswas, D.I. Gabrilovich, Characterization of the nature of granulocytic myeloid-derived suppressor cells in tumor-bearing mice, J. Leukoc. Biol. 91 (2012) 167–181, http://dx.doi.org/10.1189/jlb.0311177.
[32] R.L. He, J. Zhou, C.Z. Hanson, J. Chen, N. Cheng, R.D. Ye, Serum amyloid A induces G-CSF expression and neutrophilia via toll-like receptor 2, Blood 113 (2009) 429–437, http://dx.doi.org/10.1182/blood-2008-03-139923.
[33] X. Zhao, L. Rong, X. Zhao, X. Li, X. Liu, J. Deng, et al., TNF signaling drives myeloid-derived suppressor cell accumulation, J. Clin. Invest 122 (2012) 4094–4104, http://dx.doi.org/10.1172/JCI64115.
[34] S.P. Hu, C. Harrison, K. Xu, C.J. Cornish, C.L. Geczy, Induction of the chemotactic S100 protein, CP-10, in monocyte macrophages by lipopolysaccharide, Blood 87 (1996) 3919–3928.
[35] T. Kawai, S. Akira, Toll-like receptors and their crosstalk with other innate receptors in infection and immunity, Immunity 34 (2011) 637–650, http://dx.doi.org/10.1016/j.immuni.2011.05.006.
[36] E. Vacchelli, A. Eggermont, C. Sautès-Fridman, J. Galon, L. Zitvogel, G. Kroemer, et al., Trial watch: toll-like receptor agonists for cancer therapy, Oncoimmunol 2 (2013) e25238, http://dx.doi.org/10.4161/onci.25238.

Please cite this article in press as: A. Maruyama, et al., Pam2 lipopeptides systemically increase myeloid-derived suppressor cells through TLR2 signaling, Biochemical and Biophysical Research Communications (2015), http://dx.doi.org/10.1016/j.bbrc.2015.01.011